Analysis of robust optimization for decentralized microgrid energy management under uncertainty

Elizaveta Kuznetsova[1,2*], Carlos Ruiz[3], Yan-Fu Li[2], Enrico Zio[2,4]

[1] REEDS International Centre for Research in Ecological Economics, Eco-Innovation and Tool Development for Sustainability, University of Versailles Saint Quentin-en-Yvelines, 5-7 Boulevard d'Alembert, bâtiment d'Alembert, 78047 Guyancourt, France.

[2] Chair on Systems Science and the Energetic Challenge, European Foundation for New Energy-Electricité de France, Ecole Centrale Paris, Grande Voie des Vignes, 92295 Châtenay-Malabry, Supelec, 91190 Gif-sur-Yvette, France.

[3] Department of Statistics, Universidad Carlos III de Madrid, Avda. de la Universidad, 30, 28911-Leganes (Madrid), Spain.

[4] Dipartimento di Energia, Politecnico di Milano, Via Lambruschini 4, 20156 Milano, Italy.

* Corresponding author mailing address/Current affiliations:

Paris Saclay Energy Efficiency (PS2E), Research and Education Institute, 1, chemin de la Porte des Loges, 78354 Les Loges-en-Josas, France
Telephone: +33 (0)1 39 07 22 66
Email address: elizaveta.kuznetsova@institut-ps2e.com

Chair on Systems Science and the Energetic Challenge, European Foundation for New Energy-Electricité de France, Ecole Centrale Paris, Grande Voie des Vignes, 92295 Châtenay-Malabry, Supelec, 91190 Gif-sur-Yvette, France.
Telephone: +33 (0)1 41 13 13 07
Email address: elizaveta.kuznetsova@ecp.fr

Abstract

The present paper provides an extended analysis of a microgrid energy management framework based on Robust Optimization (RO). Uncertainties in wind power generation and energy consumption are described in the form of Prediction Intervals (PIs), estimated by a Genetic Algorithm (GA) – trained Neural Network (NN). The framework is tested and exemplified in a microgrid formed by a middle-size train station (TS) with integrated photovoltaic power production system (PV), an urban wind power plant (WPP) and a surrounding residential district (D). The system is described by Agent-Based Modelling (ABM): each stakeholder is modelled as an individual agent, which aims at a specific goal, either of decreasing its expenses from power purchasing or increasing its revenues from power selling. The aim of this paper is to identify which is the uncertainty level associated to the "extreme" conditions upon which robust management decisions perform better than a microgrid management based on expected values. This work shows how the probability of occurrence of some specific uncertain events, e.g., failures of electrical lines and electricity demand and price peaks, highly conditions the reliability and performance indicators of the microgrid under the two optimization approaches: (i) RO based on the PIs of the uncertain parameters and (ii) optimization based on expected values.

Keywords: microgrid, agent-based model, uncertain scenarios, robust optimization, power imbalance, reliability.

Nomenclature

t	time step *(h)*,
F_t^{pas}	passengers flow through TS at time *t (number/h)*,

s_t	average solar irradiation at time *t (W/m^2)*,
v_t	average wind speed at time *t (m/s)*,
E_t^l	energy required for inside and outside lighting in the train station at time *t (kWh)*,
E_t^{elev}	energy required for passengers lifting in the train station at time *t (kWh)*,
E_t^{elec}	energy required for electronic equipment in the train station at time *t (kWh)*,
E_t^{TS}	total hourly required energy in the train station at time *t (kWh)*,
E_t^D	total hourly required energy in the district at time *t (kWh)*,
P_t^{PV}	available energy output from the photovoltaic generators installed in the train station at time *t (kWh)*,
P_t^{WPP}	available energy output from the wind power plant at time *t (kWh)*,
S_t^{TS} and S_t^D	portions of energy purchased from the external grid by the TS and D, respectively (*kWh)*,
L_t^{TS} and L_t^{WPP}	portions of energy sold to the external grid by the TS and WPP, respectively *(kWh)*,
V_t^{PV} and V_t^{WPP}	portions of energy sold to the district and generated by the PV panels of the TS and WPP, respectively *(kWh)*,
R_t^{TS} and R_{t-1}^{TS}	energy levels in the train station battery at time *t* and *t-1*, respectively *(kWh)*,
R_t^D and R_{t-1}^D	energy levels in the district battery at time *t* and *t-1*, respectively *(kWh)*,
$R^{TS,stor}$	energy portion that the train station battery is capable of charging or discharging during time *t (kWh)*,
$R^{D,stor}$	energy portion that the district battery is capable of charging or discharging during time *t (kWh)*,

$\delta_t^{TS,ch}$ and $\delta_t^{TS,dis}$	binary variables which model that the train station battery can either only be charged or discharged at time *t*,
$\delta_t^{D,ch}$ and $\delta_t^{D,dis}$	binary variables which model that the district battery can either only be charged or discharged at time *t*,
$R^{TS,max}$	the maximum train station battery charge *(kWh)*,
$R^{D,max}$	the maximum district battery charge *(kWh)*,
T	time horizon considered for the optimization *(h)*,
α^{TS} and α^{D}	total costs for TS and D, respectively, for time period *T (€)*,
α^{WPP}	total revenue for WPP in time period *T (€)*,
c_t^p and c_t^s	average hourly costs of purchasing and selling *1 kWh* from the external grid, respectively, at time *t* (*€/kWh*),
c_t^D	average hourly cost per *kWh* from the bilateral contract agreed with D at time *t (€/kWh)*.
β and γ	coefficients defining the minimum amount of energy to be sold to D by TS and WPP, respectively,
$\tilde{E}_t^D$	expected energy demand for D (for the moment, considered without uncertainty) at time step *t*, predicted by TS and WPP (*kWh*),
$\tilde{V}_t^{PV}$ and $\tilde{V}_t^{WPP}$	energy portions, which TS and WPP are ready to sell to D at time step *t* (*kWh*),
$\hat{P}_t^{WPP}$	level of uncertainty quantified for the robust optimization at time *t (kWh)*,
$P_t^{WPP,ub}$ and $P_t^{WPP,lb}$	upper and lower prediction bounds of WPP power output at time *t*, respectively *(kWh)*,
τ	simulation time period composed of *Ns* time steps of one hour *(h)*,
LOLE	Loss of Load Expectation, characterizing the probability of unsatisfied electricity demand during τ,

$LOEE$	Loss of Expected Energy, quantifying the expected amount of energy losses during τ,
P_t	available capacity in the microgrid at time step *t (kWh)*,
E_t	energy demand in the microgrid at time step *t* (*kWh)*,
$Pr_t(P_t < E_t)$	probability of loss of load at time step *t*,
$E_t - P_t$	energy portion that the system is not able to supply at time step *t* (*kWh)*,
$L_t^{WPP,c}$ and $V_t^{WPP,c}$	portions of energy contracted by the WPP to the external grid and microgrid, respectively *(kWh)*,
$L_t^{WPP,*}$ and $V_t^{WPP,*}$	actual portions of energy provided by the WPP to the external grid and microgrid, respectively *(kWh)*,
T_t^{WPP}	imbalance cost generated by wind power plant at time step *t (€)*,
$d_t^{WPP,*}$	energy imbalance generated by wind power plant at time step *t (kWh)*,
$c_t^{D,+}$ and $c_t^{D,-}$	prices for positive and negative imbalances, respectively, at time step *t (€/kWh)*,
γ^C and γ^P	performance ratio calculated over a simulation period of *Ns* hours by normalizing the imbalance cost by the actual expenses / revenues calculated in the case of perfect forecast (%),
T^{hw} and T^n	constants denoting the average annual duration of high and normal wind conditions, respectively, over the time period T^{tot} *(h)*,
$\lambda^{wind}(v_t)$ and λ^{norm}	failure rates at high and normal wind conditions *(occur./y)*, respectively,
$f_v(v_t)$	weight factor caused by severe weather,
f_t^d and f_t^h	weight factors for hourly and daily variations, respectively,
r^{norm}	reference restoration time during normal weather conditions, modelled as a random variable with lognormal distribution.

1. Introduction

Renewable energies are promising solutions to the energetic and environmental challenges of the 21st century [1], [2]. Their integration into the existing grids generates technical and social challenges related to their efficient and secure management.

From this point of view, a closer location of generation and consumption sources in decentralized microgrids is expected to increase service quality for the consumers by decreasing transmission losses and the time needed to manage fault restoration and congestions. However, energy management can become critical in the microgrid, due to possible conflicting requirements or poor communication between the different microgrids elements [3]. Therefore, there is a need of frameworks for efficient microgrid energy management.

A way to model microgrids and the related individual goal-oriented decision-making of the microgrid elements is that of Agent-Based Modeling (ABM) [4]–[6], which allows analyzing by simulating the interactions among individual intelligent decision makers (the agents). The most widespread application of this modeling approach concerns the bidding strategies among individual agents, who want to increase their immediate profits through mutual negotiations and by participating in a dynamic energy market [7]–[10]. Recent studies show the extension of the ABM approach to more complex interactions in the energy management of hybrid renewable energy generation systems [6], [11], [12]. In these works, the long-term goals are focused on the efficient use of electricity within microgrids, e.g., the planning of battery scheduling to locally store the electricity generated by renewable sources and reuse it during periods of high electricity demand [11]. However, the decision framework is commonly developed under deterministic conditions, e.g., those of a typical day in summer.

To account for the variability and randomness of the operational and environmental parameters of the energy systems, several optimization techniques have been progressively introduced for handling uncertainty [13]. Fuzzy mathematical programming models and their extensions have been developed for optimal management of hybrid energy systems [14], [15]. Stochastic programming models, where the uncertain parameters are described by probability distributions, and interval programming models, where the uncertainty is described by intervals [16], [17], have been used to deal with different sources of uncertainty in optimization problems, like

economic-energy scenarios planning [18], design of renewable systems for community energy management [19], and water quality and waste management [20], [21].

In this paper, we propose an analysis of a microgrid energy management framework based on Robust Optimization (RO) previously proposed by the authors [22]. The analysis is intended to identify the conditions required for an optimal microgrid operation in presence of several sources of uncertainty, affecting the power output from renewable generators [23], the production costs [24], the electricity demand [25]. The uncertainty in the parameters is represented by Prediction Intervals (PIs), which are estimated by a Neural Network (NN), Genetic Algorithm (GA)-trained to provide lower and upper prediction bounds between which the uncertain values of the parameters are expected to lie for a given confidence level [26], [27].

The RO framework improves the reliability of the microgrid operation by selecting energy management actions that are optimal under the worst realization of the uncertainty conditions. However, this is done at the cost of possible lower revenues for the energy generators and higher expenses for the energy consumers than those that could be obtained by optimizing over the expected values of the uncertain parameters. The proposed analysis investigates the influence of uncertain events on the microgrid performance and identifies the conditions under which the application of RO or optimization based on expected values is most advantageous.

The paper is organized as follows. Section 2 motivates for the analysis carried out. Section 3 describes the models of the individual agents in the microgrid and the way that the uncertainties in the energy management parameters are accounted for. The procedure for the simulation of the uncertain scenarios and the definitions of the output quantities are discussed in Section 4 and Section 5, respectively. Section 6 applies the presented methodology to a reference microgrid system. Finally, the last section draws conclusions and gives an outlook on future research.

2. Motivation

Two optimization approaches are considered: (i) optimization based on the expected values of the uncertain quantities (also called “deterministic” optimization) and (ii) Robust Optimization (RO) based on Prediction Intervals (PIs) with a given Coverage Probability (CP).

In a previous work [22], the authors have shown that the proposed framework of RO based on PIs leads to high system reliability, but at the expense of conservative results regarding system

revenues or expenses. In fact, the proposed framework leads the decision maker to anticipate the worst possible realization of the uncertain parameters and choose the best solution with respect to such a case. By so doing, the producer plans its energy scheduling strategy by committing less energy for sale while the consumer purchases more energy than it is likely required.

The analysis proposed in this paper, aims at evaluating the system performance for different levels of uncertainty affecting both operational and environmental conditions. These uncertainties can be broadly classified in two types: (i) uncertainty related to fluctuations of the operational and environmental conditions within expected and acceptable limits. These are typical conditions for the microgrid operation, and (ii) uncertainty related to extreme events. In the first case, the fluctuations of the operational and environmental conditions can be managed by optimization based on expected parameters values without particular performance degradation [22]. In the second case RO is expected to lead to management actions that guarantee the operation within safety margins. This paper proposes methodology to simulate the uncertainty related to extreme events and to evaluate microgrid reliability and performance under different optimization approaches.

To evaluate the performance of the proposed methodology, we adopt classical reliability indicators and the so called performance ratio to quantify negative / positive imbalances caused by the prediction errors. This analysis allows showing how the probability of occurrence of an uncertain event can influence the microgrid performance indicators. Thus, this analysis provides a way of identifying the level of uncertainty in the system upon which RO performs better versus an optimization based on expected values.

3. Microgrid energy management: the practical setting

The reference system considered in this paper is the same as in [22]. It includes a middle-size train station (TS), which can play the role of power producer and consumer, the surrounding district (D) with residences and small businesses, and a small urban wind power plant (WPP). The goal of TS is to decrease its electricity expenses while satisfying its demand. To achieve this, the TS strategy includes the integration of renewable generators and energy exchanges with the local community to increase the power flexibility of the microgrid. Photovoltaic panels (PV) have been shown to be an adapted and efficient technology for its implementation on large commercial, public buildings and transportation hubs [28], [29]. For the energy exchanges with

local community, we consider only the possibility of exchange between the TS and the D. This is done to keep the model simple but also complete in order to properly illustrate the optimization analysis. Future work includes the modelling of the energy exchanges between the TS and the WPP.

The goal of WPP is to increase its revenues from selling the electricity to the external grid and to the D. The latter is considered only as an energy consumer, with the goal of decreasing its electricity purchase from the external grid by prioritizing the purchase of electricity from local sources, i.e., the TS and the WPP. In addition, we assume that the TS and the D have the capacity to store electricity in batteries.

For our current D model, we assume that the effect of locally installed renewable generators, in our case PV panels, can be neglected. The energy generated with PV panels is around 0.8% of the annual energy consumption in 2012 for the considered area [30].

Only a synthetic description of the models of the individual agents of the microgrid is presented below; for more detailed information, the interested author can refer to [22].

TS: The energy consumption E_t^{TS} *(kWh)* in the main passengers building is divided into a variable consumption, i.e. lighting and lifting depending on the solar irradiation and passengers flow, respectively, and a fixed consumption represented by plug-in electronic devices. The power required by the lifting equipment is calculated by using the methodology in [31], which is based on in-situ real time records of passengers flow. The electrical energy consumed by the lighting equipment is calculated based on the inside and outside luminosity (e.g., EN13272:2001 UK) [32]. The total energy produced by PV P_t^{PV} *(kWh)* is calculated based on the solar irradiation and technical specification of PV module [33], [34].

WPP: The total energy produced by the WPP P_t^{WPP} *(kWh)* is calculated based on the wind speed data from [35], by using the cubic correlation described in [36].

D: To simulate the energy consumption of the D, we use a top-down approach based on available statistical collections of electricity consumptions [37].

Models for the batteries charging/discharging are presented in Appendix A, i.e., eqs. (A.6) – (A.8) and eqs. (A.12) – (A.15) for the TS and D, respectively.

In this work, the market electricity price c_t^p (€/kWh) is assumed to vary following a similar trend to the wholesale market price in France [38]. Moreover, we assume that the grid offers an electricity price c_t^s *(€/kWh)* to purchase the energy from the agents. Finally, the electricity price c_t^D *(€/kWh)* is the one offered by the D to purchase the energy from the other microgrid energy producers.

As it is described in Section 2, the paper analyses the impact of different extreme events, i.e., wind storms, associated electrical lines failures and energy demand and prices peaks, on microgrid performance using two different optimization approaches: (i) optimization based on the expected values of the uncertain quantities (i.e., deterministic optimization) and (ii) RO based on PIs. The detailed formulation of the microgrid optimization problem and its solution by the two approaches is presented in Appendix A.1.

Figure 1 a,b illustrates the structure of the management scheme and operation procedure of the microgrid. The outputs from the models of the individual components are used to forecast the energy demands of the TS and D, i.e., E_t^{TS} and E_t^D, the energy outputs of the WPP and PV, i.e., P_t^{WPP} and P_t^{PV}, and the electricity prices c_t^p. These forecasted quantities feed the optimization models of the different decision-makers to determine their optimal decision variables, e.g., the battery scheduling and the energy portion to exchange between the agents and the upstream grid. In order to set up the price for the energy trading, the agents use 24-hours ahead predictions of the reference prices (c_t^p). Note that these predictions may not account for unexpected price variations.

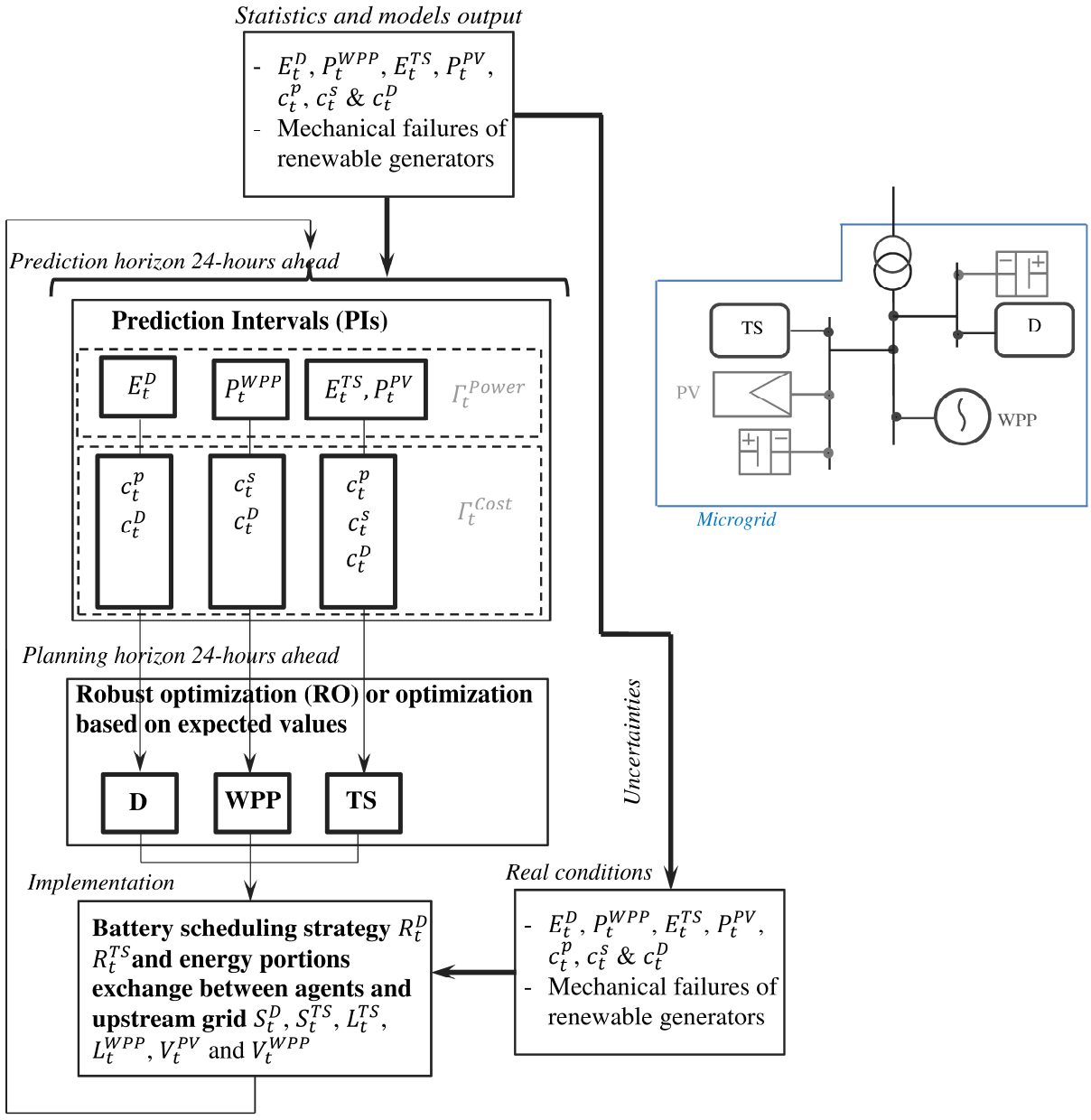
Statistics and models output
- E_t^D, P_t^{WPP}, E_t^{TS}, P_t^{PV}, c_t^p, c_t^s & c_t^D
- Mechanical failures of renewable generators
Prediction horizon 24-hours ahead
Prediction Intervals (PIs)
E_t^D
P_t^{WPP}
E_t^{TS}, P_t^{PV}
Γ_t^{Power}
c_t^p c_t^D
c_t^s c_t^D
c_t^p c_t^s c_t^D
Γ_t^{Cost}
Planning horizon 24-hours ahead
Robust optimization (RO) or optimization based on expected values
D
WPP
TS
Uncertainties
Implementation
Real conditions
Battery scheduling strategy R_t^D R_t^{TS} and energy portions exchange between agents and upstream grid S_t^D, S_t^{TS}, L_t^{TS}, L_t^{WPP}, V_t^{PV} and V_t^{WPP}
- E_t^D, P_t^{WPP}, E_t^{TS}, P_t^{PV}, c_t^p, c_t^s & c_t^D
- Mechanical failures of renewable generators
TS
D
PV
WPP
Microgrid

a)

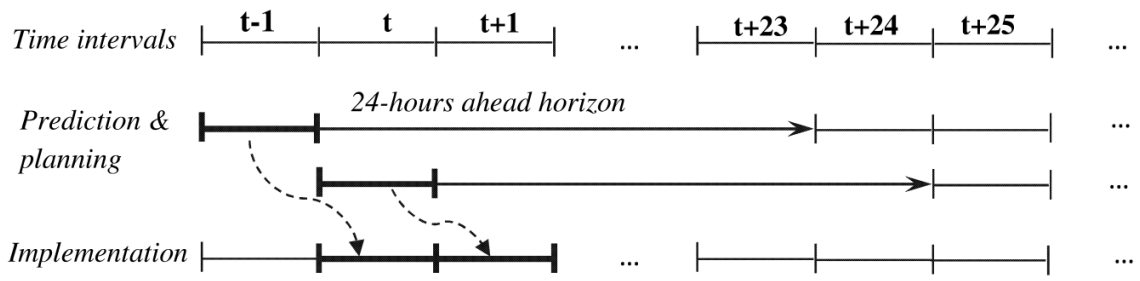

b)

Figure 1. Integrated framework: a) Structure of the management scheme; b) Operation procedure [39].

The decision-making strategy for each agent is obtained by an optimization approach so that the expenses are minimized for the D and the TS, while the revenues are maximized for the WPP. These goals are achieved through strategic battery scheduling and the optimal selection of energy exchanges between the microgrid agents and the upstream electricity grid. Thus, the consumer aims to optimize its strategy considering a time horizon of 24 time steps, each of one hour duration. Similarly, at each time *t*, the microgrid energy producers (WPP and TS) and consumer (D) have the possibility to negotiate bilateral contracts of energy exchanges to achieve their goals. Note that in this paper demand-response mechanisms for the energy management are not considered.

4. Simulation of uncertain scenarios

In order to analyse the RO framework developed in [39], we have adopted the framework illustrated in Figure 2 that allows integrating uncertain events.

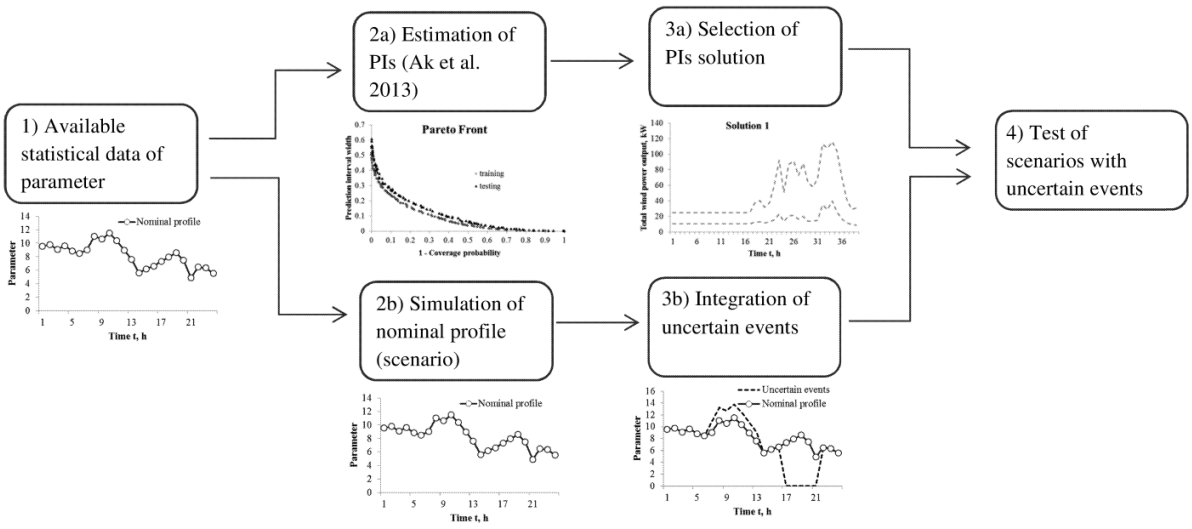

Figure 2. Procedure for construction and test of scenarios with uncertain events.

The step-by-step procedure is described in the following. The available statistical data of the parameters, such as wind power output of WPP or electricity demand for D and TS, is divided into two data sets: the first data set feeds a GA – trained NN for the estimation of the PIs; this provides a Pareto front of prediction solutions in terms of PIs with lower and upper prediction bounds between which the uncertain parameters are expected to lie with a given confidence level [27]. The second data set is used to simulate the nominal variations of the considered parameter. From the Pareto front of the available solutions, one solution of PIs can be selected according to two characteristics, i.e., Coverage Probability (CP) and Prediction Interval Width (PIW), and be used to characterize the uncertainty feasible region in the RO (eqs. (A.22) – (A.55)). In parallel, the second data set representing the nominal profile of the considered parameter is updated with uncertain events. Note that the reference to the nominal profile of the parameter indicates that it is based on historical data and does not account for any uncertain events which can arise in the future. Finally, the updated nominal profile is tested to explore the effects that the level of uncertain events may have on the microgrid performance. This is done by comparing the two management strategies for the microgrid described in Section 3, i.e., optimization based on the expected values and RO based on PIs.

The procedure for simulation of the uncertain events is briefly described in this section.

4.1. Failures correlation with environmental conditions

This section provides a brief analysis of failures of energy production installations, PV panels and wind turbines, as well as electrical lines correlated with environmental conditions in Section 4.1.1. Based on this analysis, Section 4.1.2 presents the mathematical model of electrical line failures correlation with the wind speed intensity.

4.1.1. Failures analysis

This section analyses the failures of energy production installations and electrical lines, correlated with intense environmental conditions and discusses the corresponding reliability models.

Various tests and experiments have been conducted to determine the major causes of PV panels failures, and the associated failure rates [40], [41]. Among these are thermal cycling test, humidity freeze test, damp heat test, and hot spot test, with failure rates of 15%, 14%, 10%, and 10%, respectively [40]. The effect of temperature on PV panels components, and their safety margin, have been explored in detail by taking into account different parameters, e.g., ambient temperature, irradiance, wind speed, bias conditions (open -circuit, short-circuit, maximum-power point and shading), and installation configurations (e.g., air gap between module and roof surface) [1]. Other experimentations analyse the PV panels efficiency degradation correlated with the panels temperature [42], and the application of diagnostics methods for these types of problems [43].

In reality, even if the major failure causes are known and their effects on PV panels can be diagnosed, the mathematical formulation of their correlation with temperature has not been undisputedly determined yet. Indeed, PV modules are complex multi-material energy production systems for which electrical system conditions and installation configuration play an important role. Furthermore, additional parameters, e.g., wind speed and its directions, could significantly attenuate (or change) the temperature effect on the PV panel degradation and failure behaviour, rendering them non uniform across modules of same construction and type, and with differences between test and real conditions [41].

Similarly, for wind turbines there are several statistical studies that provide information about the annual downtime and failure frequencies of wind turbine components [44]–[46]. However, the

reliability models then used, rarely address the dependence of their failure rate of wind turbines components on wind speed and other characteristics. Only few examples exist, that treat the influence of wind turbulence on rotor and pitch mechanism [45], and demonstrate that the wind turbine failure rates can be learnt by monitoring the wind characteristics [46].

Based on the above analysis, we can conclude that the definition of reliability models for multi components systems, such as those employed in energy production installation is still an open challenge. In this view, for the present research, only wind speed-correlated failures in the electrical lines have been considered. The mathematical correlations introduced allow accounting for the increase of failure frequency and repair duration times in presence of extreme environmental conditions [47].

4.1.2. Wind storms and associated failures of the electrical lines

We consider failures/repairs of the electrical lines, which are correlated with the wind speed intensity. In order to generate different profiles of wind speed, the procedure of Figure 2 is used:

1) The initial profile of wind speed is used to sample storms with different probabilities of occurrence. The continuous increase of the storms probability allows generating wind speed profiles representing different levels of uncertain conditions.
2) Each wind speed profile is analysed and the total expected failure rate and restoration time are computed.
3) The obtained failure/restoration rates are used to simulate different scenarios of uncertain events.

As described in [47], our work focuses on the simulation of wind speed-correlated failures in the overhead lines. This allows accounting for the increase of failures frequency and repair durations in presence of extreme environmental conditions [47]. The following equation defines the expected total failure rate $E\big(\lambda(v_t)\big)$:

$$E\big(\lambda(v_t)\big) = \frac{T^{hw}}{T^{tot}} \cdot \lambda^{wind}(v_t) + \frac{T^{n}}{T^{tot}} \cdot \lambda^{norm} \quad (1)$$

where T^{hw} and T^{n} are constants which denote the average annual duration (h) of high and normal wind conditions, respectively, T^{tot} is the total duration of the simulation period (h),

$\lambda^{wind}(v_t)$ and λ^{norm} are the failure rates (occur./y) at high and normal wind conditions, respectively, and α is a scaling parameter. Note that contrary to [47], we do not consider possible failures due to lightning events: therefore, eq. (1) accounts only for the increase of wind speed above a critical value. To describe the failure rate at high wind conditions, we use an exponential relationship between the failure rates of lines and wind speed:

$$\lambda^{wind}(v_t) = (\gamma_1 \cdot e^{\gamma_2 v_t} - \gamma_3) \cdot \lambda^{norm} \tag{2}$$

where v_t is the wind speed (m/s) at time *t*, $\alpha, \gamma_2, \gamma_3$ are scaling parameters and λ^{norm} is the constant failure rate during normal weather conditions. The restoration time for the overhead lines is defined as follows:

$$r_t = f_v(v_t) \cdot f_t^d \cdot f_t^h \cdot r^{norm} \tag{3}$$

where $f_v(v_t)$ is a weighting factor caused by the severe weather, f_t^d and f_t^h are weighting factors for hourly and daily variations, respectively, and r^{norm} is the reference restoration time during normal weather conditions modelled as a random variable with a lognormal distribution:

$$f_v(v_t) = \begin{cases} 1, & if\ v_t < v^{crit} \\ 1 + \frac{k \cdot (v_t - v^{crit})}{\bar{r}^{norm}}, & if\ v_t \geq v^{crit} \end{cases} \tag{4}$$

For this model, the scaling parameters and weight factors were defined through the analysis of real data in [47].

The drastic increase of the wind-caused failure rate is simulated and validated with real data for wind speeds higher than the critical one [48]. According to different studies, the critical wind speed above which the expected failure rate of the electrical lines increases is around 8 m/s [47], [48]. Based on this indication, Figure 3 *a, b* illustrates the occurrence and duration rates of discretized wind speeds for the nominal profile. The grey bars indicate normal wind speed conditions, while the black ones are related to severe wind speeds (storms) conditions.

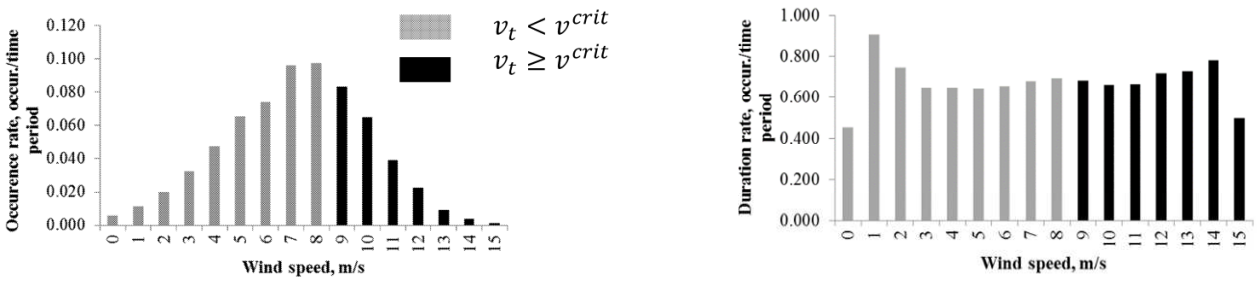

a) *b)*

Figure 3. Analysis of nominal wind speed profile: a) occurrence rate and b) duration rate of discretized wind speeds.

To analyse the influence of the wind speed intensity on the failures of electrical lines, the occurrence rate of maximum wind speed in the nominal profile is artificially raised from 0.001 to 10 occurrences per time period. To simulate the wind 'peaks', we focus on the maximum wind speed magnitude of the profile of Figure 3 a, i.e., 15 m/s. The initial occurrence rate of such wind speed magnitude has been progressively increased, as reported in Table 1. The exponential distribution is used to model the time between storms occurrence, which are considered statistically independent events [49].

Table 1. Failure and repair rates of overhead lines for different wind speed conditions.

# of wind speed profile	Wind storms		Overhead line failures	
	Occurrence rate, occur./time period	Duration rate, occur./time period	Total expected failure rate (MTTF, h), occur./time period	MTTR, h
a. Initial wind speed profile	0.001	0.5	0.5619 (3097)	2.15
b.	0.01		0.8369 (2086)	2.31
c.	0.1		3.4982 (499)	3.95
d.	1		10.3420 (168)	8.18
e.	10		11.6372 (154)	9.01

At the same time, the mean duration rate of maximum wind speed magnitude was kept unchanged and equal to 0.5 occurrences per simulation time period. This can be explained by the fact that the duration of high wind speed periods was kept as small as possible to decrease their effect on the results. Indeed, the artificial increase of wind speed raises the total energy output generated by the WPP for the considered time period. This increase of total energy output

attenuates and, in some cases, veils the effect of wind speed-correlated failures of electrical lines regarding parts of negative and positive surpluses for the long-term period.

As seen in *Table 1*, the increase of the wind storms occurrence rate generates the decrease of the MTTF and the increase of the MTTR of overhead line failures.

4.2. Energy demand and price peaks

4.2.1. Energy demand peaks

The importance to forecast the energy demand peaks and evaluate their impact on the performance and reliability of energy systems was initially emphasized in [50], and explored in other reports and scientific works for various reasons, i.e., (i) the increasing concern about electric system reliability and growing trend towards energy efficiency as a resource [51]; (ii) emergence of new market structures and opportunities for monetary compensation of sources of system reliability [51], [52]; and (iii) increased adoption of advanced metering and communication technologies that make it easier and less costly to evaluate peak demand impacts [53].

Energy demand is primarily influenced by weather conditions, i.e., temperature and hours of daylight, as well as other consumption patterns such as number of business hours and school holidays. In this view, the temperature typically drives electric demand especially among residential consumers, who can use more than half of the electricity during the peak hours of the coldest or hottest days (regulation of household temperature). However, the consumption peak can also be influenced by other parameters, e.g., special calendar events and demographics. Moreover, peaks' shifting during the day is possible during the day due to the adoption of smart grid technologies, e.g., massive plug-in of the electrical cars. Therefore, the prediction of the energy consumption patterns remains an important challenge, mainly because of the absence of sufficient amount of statistical data. For these reasons, the increase of the consumption peak occurrence and intensity are difficult to forecast with statistical models. Different works develop numerical tools to forecast the increase in energy demand peaks, e.g., statistical tools capable to capture unexpected extreme intraday increases by using available statistical records of energy demand [54], parametric models to predict long-term peaks correlated with weather, economic and demographic parameters of a particular area [55] or Bayesian estimation techniques to predict energy consumption peaks in transportation systems [56].The statistical forecast

approaches are based on the so-called normal profiles of the statistical parameter, e.g., energy consumption or temperature, which do not account for a possible increase of the peak occurrence and magnitude in the future [57]. Moreover, the multi-parameters time series models accounting for weather-induced effects, daily/weekly/yearly seasonality, special calendar events and in some cases, the variation of GDP and demographics of the geographical areas, provide a more accurate forecast for peak occurrence and magnitude [58]–[60]. Different research papers and reports [61], [62] situate the main energy demand peak timing period from noon to 6 p.m. Off-peak occurs from 9:30 p.m. to 8:30 a.m. and the rest of hours are considered to be the partial peak.

In our case, the prediction of electricity demand, which is done by using the nominal profile of the consumption, does not allow using the forecast model to simulate the increase of energy consumption peaks. The uncertainty in variations of the energy demand is, thus, artificially simulated by increasing the daily peaks during the peak hours. For this purpose, we assign the probability of peak occurrence to each day during a week by using the probabilistic approach described in [58]. According to this approach, which is validated with real statistical data, the working days, i.e., from Monday to Thursday, hold the highest probability of peak occurrence, which can vary from 0.05 to 0.15 depending on the season (Figure 1 *a*). It also provides the pdfs of the magnitude of peak electricity demand (Figure 4 *b*).

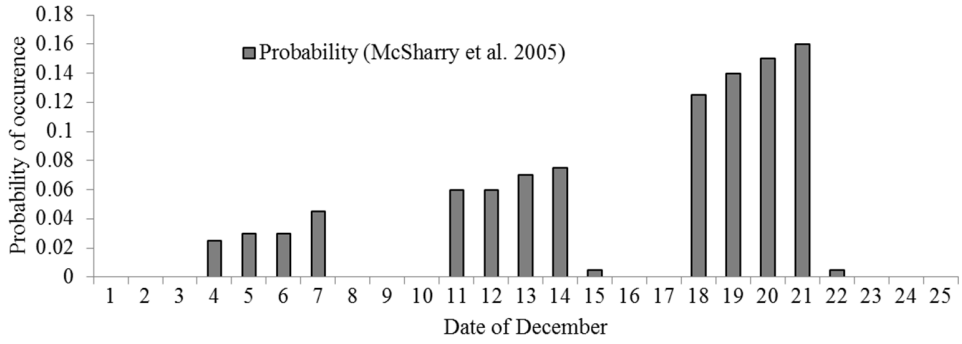

a)

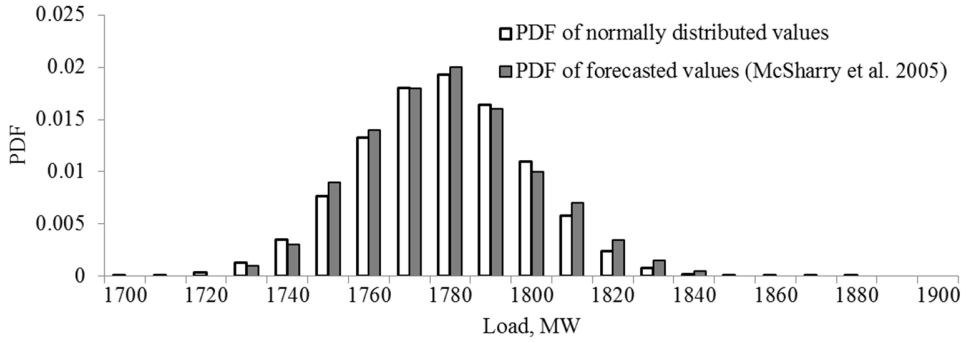

b)

Figure 4. *Example of the probabilistic forecast of the load peak year 2000* [58]*: a) Occurrence probability on various dates in December; b)pdf for forecasted values of load peak.*

Based on the conclusions presented in [58], we account for the possibility of peak occurrence only from Monday to Thursday. To generate scenarios with different levels of uncertainty in energy demand, we assign arbitrary constant values of probability of peak occurrence from Monday to Thursday, which we progressively increase, i.e., the scenarios tested here have 0.1, 0.2, 0.4, 0.6 and 0.8 probability of peak occurrence. Given the particular characteristics of the presented distribution, we assume that the peaking values of energy demand are normally distributed. In this view, the nominal value of each peak is calculated by assuming the same proportional standard deviation and a maximum value for the load peak of about 4% [58].

4.2.2. Energy price

The analysis of recent trends related to household energy bills shows a significant increase of electricity prices. For example, in the UK the increase of the energy bill is estimated to be around 20% since 2007 [63]. Moreover, the particular geographical location, implying sometimes particular microclimate conditions, as well as different electricity network configurations or energy generation portfolios, are able to generate important variations on the energy prices as it is already the case of the different UK regions [64]. In addition, the further development of Smart grids is regarded to be a main driver of the increase of the household energy bills [63].

However, even in countries with strong electricity markets, where producers, consumers and transmission companies are involved in the price formulation, the correlation between energy demand and price remains important (e.g., 0.58 for UK). Indeed, important investments, that are

directed to upgrade the existing infrastructure to help the network support demand during peak times and to avoid power outages, are one of the causes of the increase of electricity prices. Therefore, in this paper the increase of the energy demand peaks is explored jointly with the increase of the electricity market price especially when the variations in market electricity prices allow following the trend of the energy demand curve, i.e., during working days rather than during weekends.

This increase of the energy demand peaks is assumed to be followed by an increase in the electricity price from the upstream grid. The electricity tariff from the external grid adopted for this case study is a tariff structure for commercial utilization, which is made up of a basic charge, a daytime unit rate, a night unit rate and a peak charge. This tariff is introduced in [61] and adopted in [65]. By assuming that the energy demand of the district E_t^D follows the same trend than the energy demand profile in the upstream grid, we can adopt a similar assumption regarding the proportional correlation between the daily electricity market price and the daily energy demand [61], [65], [66].This is done to simulate the variations in the upstream market price. However, it is important to highlight that during the peaks of electricity demand, the electricity price can be no longer proportional to demand, but rise drastically. This Critical Peak Price (CPP) represents a dynamic rate that is dispatched for the utilities based on real-time capacity conditions. The value of the critical peak price is several times higher than the usual price applied during the off-peak periods, e.g., CPP rate is 6 - 7 for [67], [68]. The objective of this price increase can be to reduce the electricity consumption during critical times [67], [69]. In this paper, we are not focussing on demand-response management techniques, but on evaluating the expenses paid by the consumers in case of an inaccurate prediction of the energy consumption. For this, we have tested different values of the critical peak price, applied during the peak period from noon to 6 p.m.

5. Output indicators

In this section we present the indicators used to evaluate microgrid performance and reliability.

5.1.Microgrid reliability

The overall microgrid performance is evaluated in terms of classical adequacy assessment metrics, which characterize the ability of the DG system energy capacity to meet system demand in presence of uncertainty [70]. Specifically, Loss of Load Expectation (LOLE) is used to

characterize the probability of unsatisfied electricity demand and Loss of Expected Energy (LOEE) to quantify the expected amount of energy losses for *Ns* time steps of one hour:

$$LOLE = \sum_{t=0}^{Ns} Pr_t(P_t < E_t) \tag{5}$$

$$LOEE = \sum_{t=0}^{Ns} Pr_t(P_t < E_t) \cdot (E_t - P_t) \tag{6}$$

where $Pr_t(P_t < E_t)$ is the probability of loss of load at time step *t*, P_t *(kWh)* is the available capacity at time period *t*, E_t *(kWh)* is the energy demand at time step *t*, in our case defined as follows:

$$P_t = S_t^D + S_t^{TS} + V_t^{PV} + V_t^{WPP} + \delta_t^{D,dis} \cdot R^{D,stor} + \delta_t^{TS,dis} \cdot R^{TS,stor} \qquad \forall t \tag{7}$$

$$E_t = E_t^D + E_t^{TS} + \delta_t^{D,ch} \cdot R^{D,stor} + \delta_t^{TS,ch} \cdot R^{TS,stor} \qquad \forall t \tag{8}$$

The available power capacity of the microgrid P_t (eq. 7) represents the sum of the electricity produced by all generation units at time step *t*. In our case, P_t accounts for the amount of energy purchased from the external grid (i.e., S_t^D and S_t^{TS}), produced by the local generators (i.e., V_t^{PV} and V_t^{WPP}) and discharged from the batteries (i.e., $\delta_t^{D,dis} \cdot R^{D,stor}$ and $\delta_t^{TS,dis} \cdot R^{TS,stor}$).

5.2. Microgrid imbalance

The renewable generators installed in the microgrid, i.e., WPP and PV power production in TS, are committed to provide V_t^{WPP} and V_t^{PV} to the D, and L_t^{WPP} and L_t^{PV} to the upstream grid. The non-supplied energy can generate reliability problems for the microgrid and the upstream grid. By taking into account the prediction errors and/or the mechanical failures of the renewable generators, their common revenues for time step *t* are formulated as:

$$\alpha_t^{\Sigma,\mathrm{P}} = (L_t^{WPP,c} + L_t^{PV,c}) \cdot c_t^S + (V_t^{WPP,c} + V_t^{PV,c}) \cdot c_t^D + T_t^{\Sigma,\mathrm{P}} \qquad \forall t \tag{9}$$

where $L_t^{WPP,c}$, $L_t^{PV,c}$, $V_t^{WPP,c}$ and $V_t^{PV,c}$ *(kWh)* are the contracted amounts of energy provided by the WPP and PV to the external grid and microgrid, respectively, $T_t^{\Sigma,\mathrm{P}}$ *(€)* is the imbalance cost of the renewable generators defined as follows:

$$T_t^{\Sigma,\mathrm{P}} = (d_t^{L_t^{WPP,*}} + d_t^{L_t^{PV,*}}) \cdot c_t^{s,+/-} + (d_t^{V_t^{WPP,*}} + d_t^{V_t^{PV,*}}) \cdot c_t^{D,+/-} \tag{10}$$

where $d_t^{V_t^{WPP,*}}$, $d_t^{V_t^{PV,*}}$, $d_t^{L_t^{WPP,*}}$ and $d_t^{L_t^{PV,*}}$ *(kWh)* are the imbalances for time step *t* calculated as the difference between the actual amount of energy *(kWh)* that the renewable generator can

supply and the level of contracted energy *(kWh)*. The prices $c_t^{D,+/-}$ and $c_t^{s,+/-}$ *(€/kWh)* are the imbalance prices for positive and negative imbalances, respectively, at time step *t*.

Note that the expenses of D are defined similar to the revenues of the renewable generators:

$$\alpha_t^{\Sigma,\mathrm{C}} = S_t^{D,c} \cdot c_t^p + (V_t^{WPP,c} + V_t^{PV,c}) \cdot c_t^D + T_t^{\Sigma,\mathrm{C}} \qquad \forall t \qquad (11)$$

where $S_t^{D,c}$, $V_t^{WPP,c}$ and $V_t^{PV,c}$ *(kWh)* are the contracted amounts of energy from the external grid and local renewable generators, respectively, and $T_t^{\Sigma,\mathrm{C}}$ *(€)* is the cost paid to supply the peak electricity demand.

Again, note that the formulation of revenues accounting for the imbalance cost is done for contract durations of one hour.

To define the formulation of the imbalance prices, we have reviewed the existing imbalance tariff structures and regulation mechanism of European countries [71] such as Belgium, Netherland, France and Spain. Among the existing formulations, the definition of imbalance price in Spain is taken as example because of its simplicity, whereby the imbalance price is equal to a certain proportion of the spot price [72], [73]. In the numerical application that follows (Section 6), we have tested different imbalance prices to analyse the influence on the performance.

To evaluate the impact of the imbalance cost on the renewable generators revenues, we introduce the performance ratio γ^P (eq. 12), which is calculated over a simulation period of *Ns* hours. Note that γ^P is computed by normalizing the total imbalance cost generated by the renewable generators by the revenues that would be obtained in the case of a perfect forecast [72]. To evaluate the impact of the load and price peaks, the coefficient γ^C (eq. 13) is calculated similar to γ^P, i.e., normalizing the imbalance cost generated during the peaking periods by the expenses that D would pay in case of a perfect forecast:

$$\gamma^P = \left(1 - \frac{\sum_{t=0}^{Ns} \left|T_t^{\Sigma,\mathrm{P}}\right|}{\sum_{t=0}^{Ns} \left[(L_t^{WPP,c} + L_t^{PV,c}) \cdot c_t^s + (V_t^{WPP,c} + V_t^{PV,c}) \cdot c_t^D\right]}\right) \cdot 100\% \qquad (12)$$

$$\gamma^C = \left(1 - \frac{\sum_{t=0}^{Ns} \left|T_t^{\Sigma,\mathrm{C}}\right|}{\sum_{t=0}^{Ns} \left[S_t^{D,c} \cdot c_t^p + (V_t^{WPP,c} + V_t^{PV,c}) \cdot c_t^D\right]}\right) \cdot 100\% \qquad (13)$$

The proposed performance ratios are expressed in percentage, i.e., $\gamma^P, \gamma^C \in (0,100]$. For perfect predictions, i.e., when deviations from committed energy are null, performance ratios are 100%.

In general, microgrids can operated in two modes: the grid-connected mode and the islanded mode. In the grid-connected mode, the microgrid can trade power with the upstream power grid to solve the power imbalance. On the other hand, power imbalances in the islanded mode can be solved by decreasing the total output of the distributed generators (DGs), or by load-shedding, which is an intentional load reduction [74]. In our paper, we focus on the grid-connected mode. Therefore, the power imbalances are accounted inside the microgrid and between the microgrid power producers and the upstream external grid.

6. Numerical case study

As discussed in Subsection 3.3, the PIs of the available wind energy output P_t^{WPP}, and energy demands E_t^{TS} and E_t^D are estimated by a NN trained by a NSGA-II with respect to two objectives: the coverage of the prediction interval (to be maximized) and their width (to be minimized) [27]. This optimization gives rise to the Pareto fronts depicted in Figure 5, from which different solutions can be selected and used in the energy management by RO. Note that these solutions differs on the interval widths and on their corresponding coverage probability and were also used in paper [39].

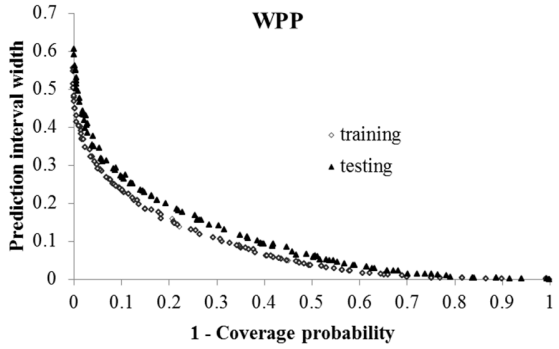

a)

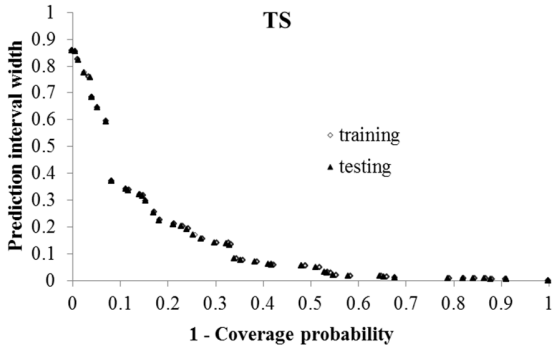

b)

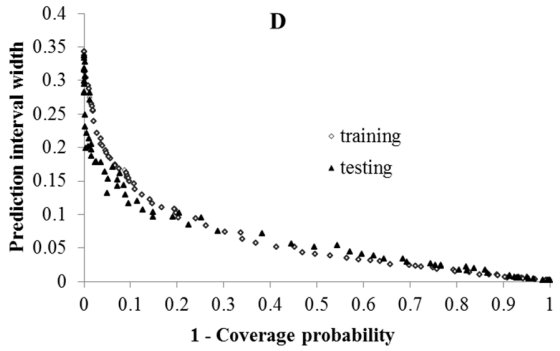

c)

Figure 5. *Pareto fronts of PIs: a)* P_t^{WPP}*, b)* E_t^{TS} *and c)* E_t^D.

The comparison of the optimization results obtained with the RO based on PIs with (i) CP = 96% and (ii) CP = 56.3% shows that PIs with high CP decrease drastically the amount of committed energy [39]. This is due to the large width of the PIs characterized by high CP, i.e., 96%, which forces the RO to provide a very conservative solution. As a consequence, the producer plans its energy scheduling strategy based on the worst possible realization of the available power production and thus commits less energy for sale; at the opposite, the consumer anticipates the worst possible realization of its uncertain consumption and, thus, it purchases more energy than it will probably be required in the future. As a consequence the performance ratio of the RO based on the PIs with high CP = 96% is very low. On the contrary, the optimization based on the PIs with low CP = 56.3% considers “less extreme” worst realizations and, thus, provides adequate results in terms of performance ratio, comparable with results of other optimization techniques [72], and achieves satisfactory values of the reliability indicators, i.e., LOLE and LOEE, in comparison with these achieved by the optimization based on expected values.

In this view, for the following we consider and analyse the performance of the RO based on the PIs with moderate CP in the range of 50 – 60%. The PIs used for the prediction of the electricity power output are selected from the Pareto front (Figure 5 *a*) of the available solutions, with prediction interval width (PIW) and coverage probability (CP) equal to 0.0535 and 56%, respectively. The PIs used for the electricity demand prediction are selected from the Pareto front (Figure 5 *c*) of the available solutions with similar characteristics than the PIs used for the wind power output prediction, i.e., PIW = 0.0518 and CP = 50.5%.

To account for the variations of the electricity prices c_t^p, c_t^s and c_t^D, the lower and upper bounds of their associated PIs have been assumed to be the ±10% of their expected values. Similarly, the variations of P_t^{PV} have been accounted for by setting the lower and upper bounds of the PIs to ±5% of their expected values. Note that these PIs widths have been fixed based on the accuracy of a 24-hours ahead prediction for the electricity prices [75] and the PV energy output [76]. The optimization based on the expected values has been performed also; as it was discussed in Appendix A.1, by considering the mean of the prediction interval as a point estimate of the uncertain quantity of interest. Note that the effect of the electrical lines failures and the increase of the energy demand and prices peaks will be explored separately from each other.

6.1. Impact of wind storms and associated lines failures

Based on Table 1, five case studies are considered under the following assumptions:

- Failures of the electrical lines are considered to occur within the microgrid.
- The same initial wind speed profile was used for the sampling of overhead line failures with different MTTF and MTTR. Indeed, the use of the wind speed profiles with the artificially increased wind speeds for the different case studies, renders a higher wind power output and, consequently, the performance ratio over the simulation period is increased. This disturbs the output indicators, such as the performance ratio, by hiding the effect of the overhead lines failures.
- The failures/repair rates of the generation units inside the microgrid, i.e., PV and WPP, are considered constant and of the same values as in [39].

For the point estimation of the wind energy output P_t^{WPP}, which is used for the optimization based on the expected values, we use the mean of the considered prediction interval with CP = 56.3%. The results obtained by the simulation of the agents dynamics on a period of $\tau = 1680\,h$ have been calculated as the average over *Ns = 20* simulations, which is a sufficiently large number of simulations to efficiently determine the convergence of the different indicators. The convergence is evaluated by considering the difference between two successive values of the indicators moving average where a threshold value of 2% is used.

Figure 6 *a,b* shows the variations of the shortage and surplus in percentage of the total amount of committed energy under different conditions of failures and repairs using the RO and the optimization based on expected values.

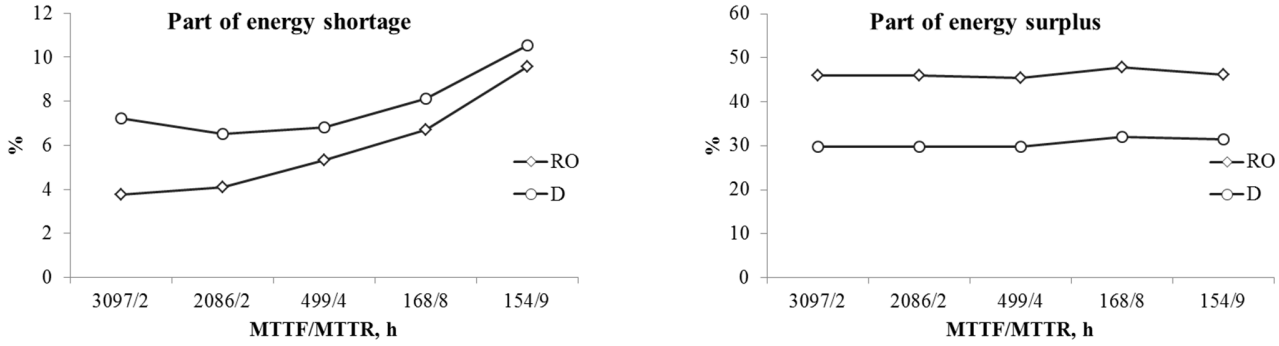

a) *b)*

Figure 6. *Variations of shortage and surplus proportions in percentage of the total amount of committed energy using RO based on the PIs and deterministic optimization based on the expected values: a) Shortage; b) Surplus.*

As it can be observed in Figure 6 *a,b*, the increase of the MTTF associated to the electrical lines increases the number of shortages in the grid, and this is common to both optimization approaches. With the increase of the probability of electrical lines failure, i.e., of the ratio MTTF/MTTR, the proportions of shortage tend to the values 9.59% and 10.54% for RO based on the PIs and optimization based on the expected values, respectively. This indicates that the RO based on the PIs with moderate CP efficiently account for shortage up to a certain level of the probability of the uncertain events occurrence. Note that the energy shortage due to large failure rates of the electrical lines optimized by RO based on PIs tends to the results provided by the optimization based on expected values. In order to increase the robustness to failures, PIs with higher CP would have to be used.

At the same time, the surplus caused by the low available wind power used by the RO remains almost the same, with a minor increase of about 1% between a MTTF/MTTR of 3097/2 and 154/9, respectively. This increase is due to the increase of the electrical line failures between D and the other microgrid players, which results in the rise of the energy surplus in the microgrid.

It is important to highlight that the RO based on the PIs is generally characterized by smaller shortages and a higher surpluses than the optimization based on the expected values.

Due to the particular characteristics and data of the case study considered in this paper, the negative imbalance is smaller than the positive imbalance. In this view, the variations in the negative imbalance generate a small impact on the performance ratios (12) and (13), which show a decrease of 0.66 and 1.02% between a MTTF/MTTR of 3097/2 and 154/9, for the RO based on the PIs and the optimization based on the expected values, respectively. Note that the surplus and shortage values depend on different microgrid parameters, i.e., the microgrid structure and characteristics, strategy of the agents, optimization constraints, etc. In this view, the higher the shortage the higher impact on the performance ratios, especially for the optimization based on the expected values, which is more sensible to the negative imbalances.

Table 2. *Performance ratios γ^P of the RO based on PIs and the optimization based on the expected values.*

%		10	20	40	60	80	100	120	140	160	180	200	220	240
3097/2	RO	97	96.6	**95.7**	**94.9**	**94.1**	**93.2**	**92.4**	**91.6**	**90.7**	**89.9**	**89.0**	**88.2**	**87.4**
	D	97.5	96.7	95.2	93.6	92	90.4	88.8	87.2	85.6	84	82.4	80.8	79.2
154/9	RO	96.4	95.2	93.3	91.2	**89.2**	**87.1**	**85**	**83**	**80.9**	**78.9**	**76.8**	**74.7**	**73.1**
	D	97.1	95.7	93.7	91.4	89.1	86.8	84.6	82.3	80	77.7	75.4	73.2	70.9

Table 2 provides the information about the values of the performance ratios γ^P of the RO based on the PIs and the optimization based on the expected values obtained for the two extreme scenarios presented in Table 2, i.e., MTTF/MTTR of 3097/2 and 154/9, respectively. As it can be observed, both optimization approaches provide good performance, which is comparable to the performances of different approaches tested in [72]. The RO based on the PIs becomes more advantageous with the increase of the negative imbalance price (bold values).

Based on the results in Table 2, the variation of the performance ratio γ^P depends not only on the energy shortage and surplus, but also on the spot and upstream electricity prices. Figure 7 illustrates the variation of the difference between the performance ratios obtained for the RO based on the PIs and the optimization based on the expected value for two extreme scenarios, i.e., MTTF/MTTR of 3097/2 and 154/9, respectively. Note that in Figure 7 the percentage of the price for the positive imbalance is considered to be 5% of the spot price. The Standard Deviation

(SD) is used to quantify the uncertainty of the performance ratios in the *Ns = 20* scenarios summarized in Table 1.

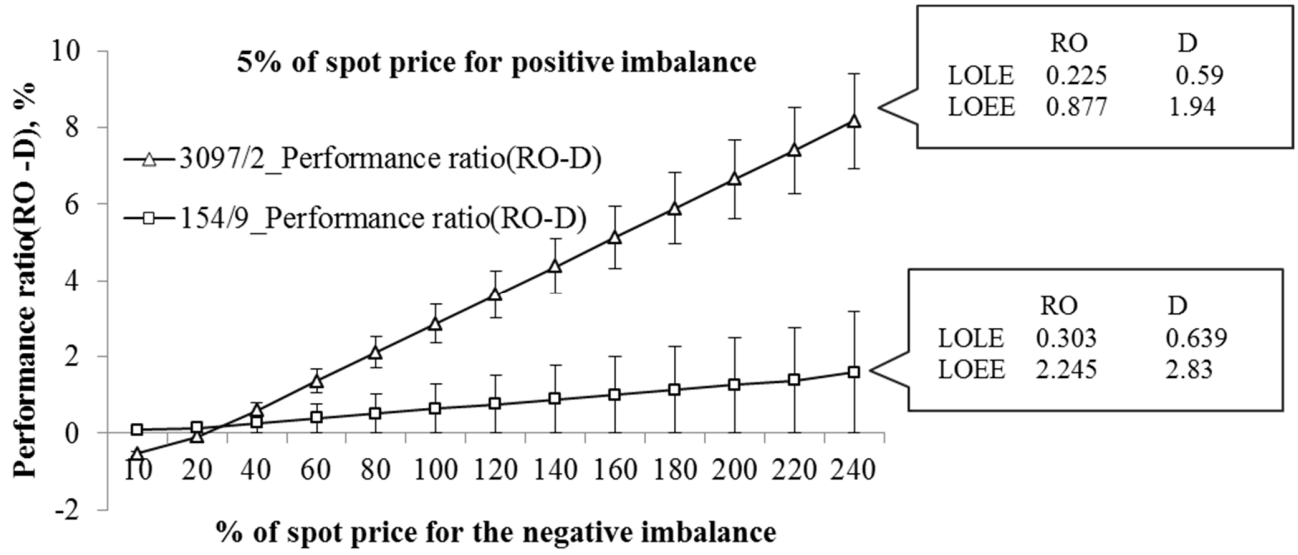

Figure 7. *Performance ratio γ^P differences for RO based on PIs and optimization based on the expected values.*

It can be observed that with the increase of the negative imbalance price, the network optimized by RO based on the PIs gains in profitability in terms of performance ratio. This profitability is even more evident for the case of MTTF/MTTR = 3097/2. For the case of MTTF/MTTR = 154/9, the performance ratio of the RO based on the PIs shows a small increase and remains close to the performance ratio obtained with the optimization based on the expected values. According to the reliability indicators, shown for the two considered scenarios in the right part of Figure 7, the RO based on the PIs holds the lowest LOLE and LOEE for both scenarios. The increase of MTTF from 3097 to 154 h decreases the reliability indicators for both optimization approaches. However, the RO based on the PIs is more reliable in comparison with the optimization based on the expected values.

Figure 8 *a-d* shows the variation of the performance ratio in a three-dimensional coordinate system defined by the following axes: percentage of the negative imbalance price (%), MTTF/MTTR (h) and the difference between the performance ratio values calculated for the RO based on the PIs and the optimization based on the expected values (%). The performance ratio

difference provides a visual illustration of the profitability for the two approaches: the white bars (negative values) show the advantage to use the optimization based on the expected values over the RO based on the PIs and the grey bars (positive values) indicates a better performance of the RO based on the PIs. Each figure plots different values for the positive imbalance prices.

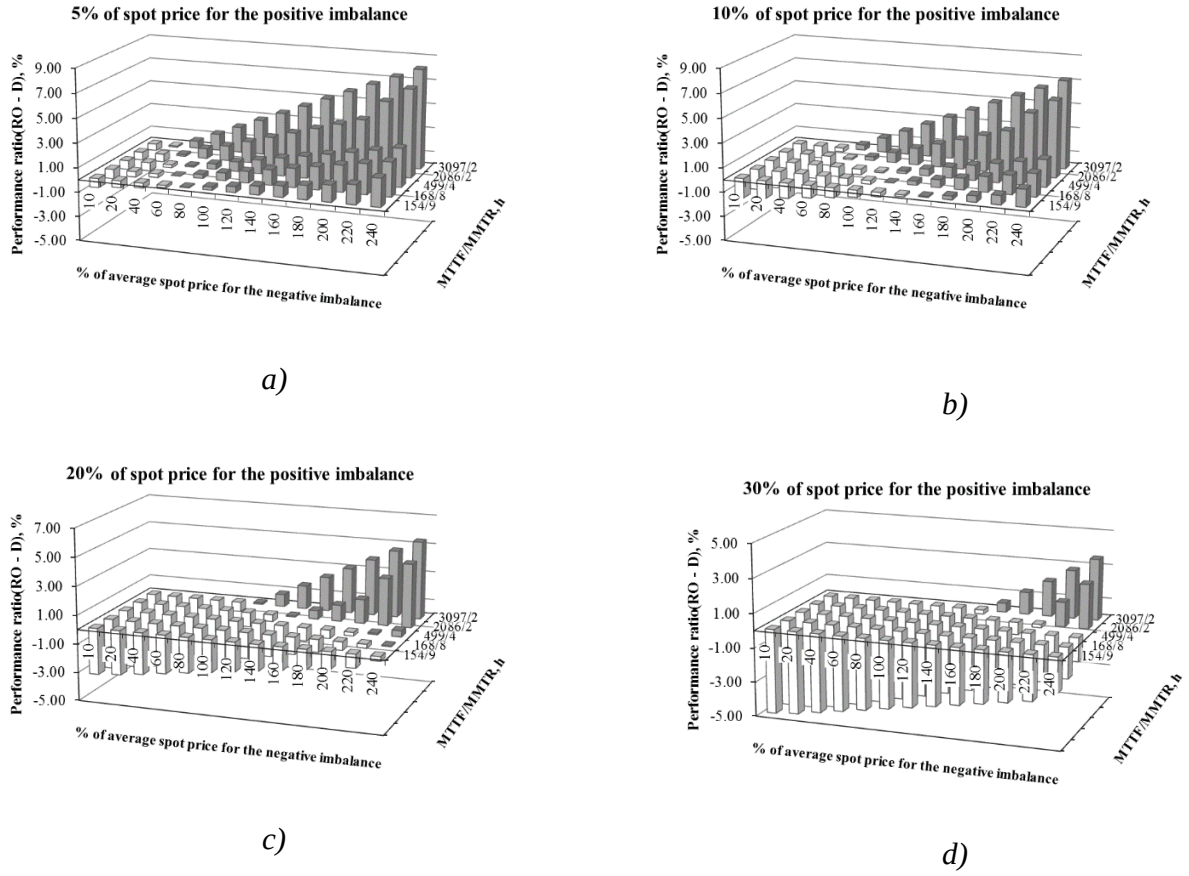

Figure 8. *Performance ratio differences for RO based on PIs and the optimization based on the expected values depending on the negative imbalance price and MTTF/MTTR for different percentages of spot price for the positive imbalance: a) 5%; b) 10%; c) 20%; d) 30%.*

As it can be observed in Figure 8 *a*, the increase of the negative imbalance price makes the use of the RO based on the PIs more profitable in terms of the performance ratio (starting with 40% of average spot price for the negative imbalance). This profitability becomes significant as the rates of failures occurrence are lower, i.e., MTTF/MTTR = 3097/2 h. Note that the advantage of RO slightly decreases with the increase of the MTTF of the electrical lines due to the increase of the negative imbalance part (cf. Figure 8 *a*). The increase of the positive imbalance price

compensates progressively the penalty paid for the negative imbalance and reduces the advantage of the RO based on the PIs.

We have to underline once again that the performance ratio characterizes the microgrid revenues in presence of negative and positive imbalances. However, these results highly depend on the election on the model parameters, i.e., the microgrid structure and characteristics, strategy of the agents, optimization constraints, etc.

6.2. Impact of energy demand and prices peaks

We tested different values of the peak price applied during the peak periods, i.e., from noon to 6 p.m. Table 3 recalls the performance ratios γ^C of the RO based on the PIs and the optimization based on expected values obtained for two extreme peak occurrence probability scenarios: 0.1 and 0.8.

Table 3. *Performance ratios and reliability indicators for the RO based on PIs and the optimization based on expected values.*

%/ CPP rate			1	2	4	6	8
Probability of peak occurrence	0.1	RO	94.56	94.35	93.94	**93.54**	**93.16**
		D	95.74	95.23	94.29	93.44	92.66
	0.8	RO	92.3	**90.33**	**87.7**	**86.02**	**84.85**
		D	92.51	89.87	86.57	84.58	83.25

As it can the observed, the increase of the probability of peak occurrence generates a decrease of the performance ratio γ^C. Additionally, the increase of the CPP rate degrades the performance ratio for both RO based on the PIs and the optimization based on the expected values. It can be noticed that the RO based on the PIs becomes more advantageous with the increase of the CPP rate (bold values).

Figure 9 illustrates the influence of the progressive increase of the probability of the load peak occurrence on the output indicators.

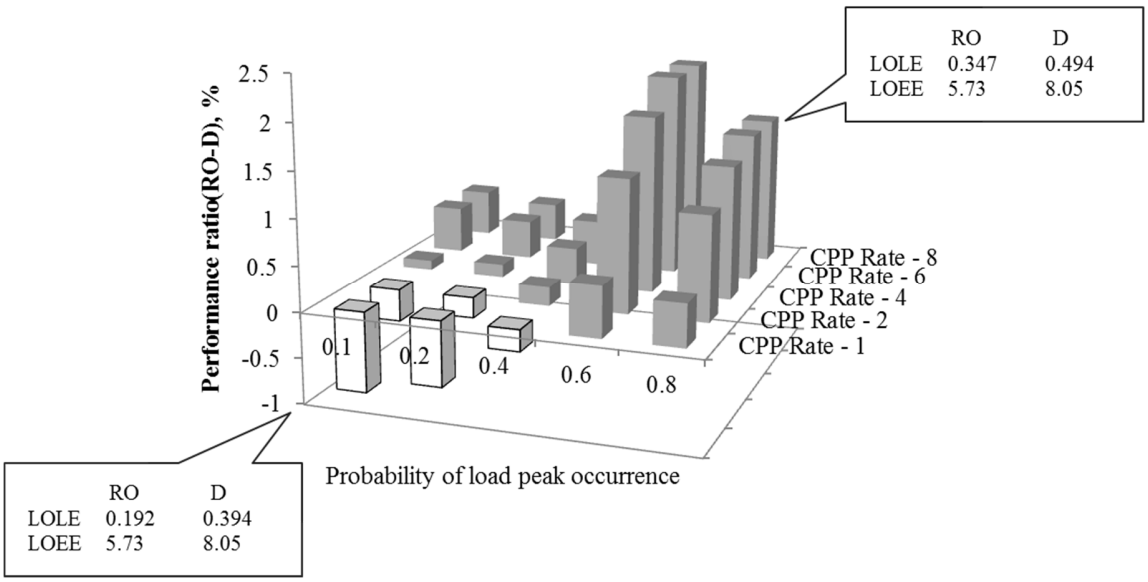

Figure 9. *Performance ratio γ^C differences for RO based on PIs and optimization based on the expected value.*

It can be observed, that with the increase of the probability of peak occurrence, the RO based on the PIs performs better in terms of the performance ratio γ^C. This profitability is even more evident for the case of a maximum CPP rate. Moreover, the peak of profitability for the RO is situated at a probability of peak occurrence of 0.6. The progressive increase of the probability of peak occurrence will decrease the performance ratio γ^C obtained with the RO. According to the reliability indicators, shown for two extreme scenarios of 0.1 and 0.8 of probability of peak occurrence, the RO based on the PIs holds the lowest LOLE and LOEE for both scenarios. The increase of probability of peak occurrence from 0.1 to 0.8 degrades the reliability indicators for both optimization approaches. However, the RO based on the PIs is more reliable in comparison with the optimization based on the expected values.

7. Conclusions

The present paper provides an extended analysis of microgrid energy management under two optimization frameworks: Robust Optimization (RO) based on Prediction Intervals (PIs) and optimization based on expected values. The considered frameworks are exemplified on a microgrid including the following stakeholders: a middle-size train station (TS) with integrated

photovoltaic power production system (PV), a urban wind power plant (WPP), and a surrounding residential district (D). The system is described by Agent-Based Modelling (ABM), in which each stakeholder, modelled as an individual agent, aims at a particular goal, i.e., decreasing its expenses from power purchases or increasing its revenues from power selling.

The proposed analysis allows evaluating the impact of different levels of uncertainty on the agent expense and revenue functions, as well as on the overall microgrid reliability. Furthermore, the imbalance cost has been introduced to quantify the effect of prediction errors and failure occurrences. The analysis shows how the probability of occurrence of some specific uncertain events, e.g. failures of electrical lines and electricity demand and price peaks, highly conditions the reliability and the performance indicators of the microgrid under the two optimization approaches: RO based on the PIs and optimization based on expected values.

In particular, the proposed methodology allows identifying the level of uncertainty in the operational and environmental conditions upon which RO performs better than an optimization based on expected values.

This analysis is intended to assist decision-makers to select microgrid energy management actions that provide an adequate trade-off between system reliability and economic performance.

Regarding the results obtained in the numerical case study considered, the following conclusions are in order:

- The reliability analysis performed for different levels of wind power output uncertainty shows a strong improvement on the reliability indicators if RO based on the PIs is used
- As it was expected, the increase of the probabilities of uncertain events, i.e., failure of electrical lines, frequency of electricity peaks and increase of electricity price during peak-hours, shows the advantage of RO based on the PIs in comparison with an optimization based on the expected values.
- The price variations play a significant role in the system's performance. In particular, with an increase of either the price for the negative imbalance or the peak-hours price, the RO shows a clear advantage in comparison with the optimization based on expected values. Thus, there is a threshold probability of uncertain events occurrence above which RO based on PIs performs better, which strongly depends on the price variations.

- In addition, there is a second threshold probability that indicates some limitations of the RO based on the PIs. In particular, the PIs considered in this paper, which are obtained from a CP of about 50% , efficient up to certain level of the probability of the uncertain events occurrence.

The adoption of RO based on the PIs or optimization based on expected values must be guided by the knowledge on the environmental and operational conditions of the microgrid under study. Future research will consider the development of hybrid optimization frameworks, for switching between different optimization techniques by considering the different environmental and operational conditions of the microgrid that may be expected at different times.

Acknowledgments

The authors acknowledge the support of the Chair on Systems Science and the Energetic Challenge, European Foundation for New Energy - Electricité de France (EDF) at Ecole Centrale Paris and Supelec.

The authors also wish to thank the anonymous referees for their scrupulous review work and the comments provided to us, which have helped improving the paper significantly.

Appendix A

A.1. Optimization framework

For completeness of the paper, we present the optimization problem as considered in [22] and here taken for our analysis. The decision-making strategy for each agent, identified by the use of robust optimization, is based on the expenses minimization for the district (D) and train station (TS) and the revenues maximization for the wind power plant (WPP). For the purpose of better understanding here below the deterministic and the RO problems are presented.

A.1.1. Deterministic optimization problem

The optimization of energy scheduling for the TS, WPP and D, where the objective functions to be optimized are formulated in terms of expenses for the TS (eq.A.2) and D (eq.A.11), and revenues for the WPP (eq.A.19), are posed as follows.

Optimization problem - TS

Minimize $\boldsymbol{\alpha^{TS}}$

s.t.

$$E_t^{TS} + L_t^{TS} + \delta_t^{TS,ch} \cdot R^{TS,stor} - \delta_t^{TS,dis} \cdot R^{TS,stor} + V_t^{PV} \leq P_t^{PV} + S_t^{TS} \qquad \forall t \qquad \text{(A.1)}$$

$$\sum_{t=0}^{T} (c_t^p \cdot S_t^{TS} - c_t^s \cdot L_t^{TS} - c_t^D \cdot V_t^{PV}) \leq \alpha^{TS} \qquad \text{(A.2)}$$

$$L_t^{TS} + V_t^{PV} \leq P_t^{PV} \qquad \forall t \qquad \text{(A.3)}$$

$$S_t^{TS} \geq 0, L_t^{TS} \geq 0, V_t^{PV} \geq 0 \qquad \forall t \qquad \text{(A.4)}$$

$$\begin{cases} \beta \cdot \tilde{E}_t^D \leq V_t^{PV}, & if\ P_t^{PV} \geq \beta \cdot \tilde{E}_t^D \\ 0 \leq V_t^{PV}, & otherwise \end{cases} \qquad \forall t \qquad \text{(A.5)}$$

$$R_t^{TS} \leq R_{t-1}^{TS} + \delta_t^{TS,ch} \cdot R^{TS,stor} - \delta_t^{TS,dis} \cdot R^{TS,stor} \qquad \forall t \qquad \text{(A.6)}$$

$$\delta_t^{TS,ch} + \delta_t^{TS,dis} \leq 1 \qquad \forall t \qquad \text{(A.7)}$$

$$0 \leq \delta_t^{TS,ch} \leq 1, 0 \leq \delta_t^{TS,dis} \leq 1 \qquad \forall t \qquad \text{(A.8)}$$

$$0 \leq R_t^{TS} \leq R^{TS,max} \qquad \forall t \qquad \text{(A.9)}$$

Optimization problem - D

Minimize $\boldsymbol{\alpha^D}$

s.t.

$$E_t^D \leq S_t^D + V_t^{PV} + V_t^{WPP} - (\delta_t^{D,ch} \cdot R^{D,stor} - \delta_t^{D,dis} \cdot R^{D,stor}) \qquad \forall t \qquad \text{(A.10)}$$

$$\sum_{t=0}^{T} (c_t^p \cdot S_t^D + c_t^D \cdot V_t^{WPP} + c_t^D \cdot V_t^{PV}) \leq \alpha^D \qquad \text{(A.11)}$$

$$R_t^D \leq R_{t-1}^D + \delta_t^{D,ch} \cdot R^{D,stor} - \delta_t^{D,dis} \cdot R^{D,stor} \qquad \forall t \qquad \text{(A.12)}$$

$$\delta_t^{D,ch} + \delta_t^{D,dis} \leq 1 \qquad \forall t \qquad \text{(A.13)}$$

$$0 \leq \delta_t^{D,ch} \leq 1, 0 \leq \delta_t^{D,dis} \leq 1 \qquad \forall t \qquad \text{(A.14)}$$

$$0 \leq R_t^D \leq R^{D,max} \qquad \forall t \qquad \text{(A.15)}$$

$$S_t^D \geq 0 \qquad \forall t \qquad \text{(A.16)}$$

$$V_t^{PV} = \tilde{V}_t^{PV}, V_t^{WPP} = \tilde{V}_t^{WPP} \qquad \forall t \qquad \text{(A.17)}$$

Optimization problem - WPP

Maximize $\boldsymbol{\alpha^{WPP}}$

s.t.

$$L_t^{WPP} + V_t^{WPP} \leq P_t^{WPP} \qquad \forall t \qquad \text{(A.18)}$$

$$\sum_{t=0}^{T}(c_t^s \cdot L_t^{WPP} + c_t^D \cdot V_t^{WPP}) \geq \alpha^{WPP} \qquad \text{(A.19)}$$

$$\begin{cases} \gamma \cdot \tilde{E}_t^D \leq V_t^{WPP}, & if\ P_t^{WPP} \geq \gamma \cdot \tilde{E}_t^D \\ 0 \leq V_t^{WPP}, & otherwise \end{cases} \qquad \forall t \qquad \text{(A.20)}$$

$$L_t^{WPP} \geq 0, V_t^{WPP} \geq 0 \qquad \forall t \qquad \text{(A.21)}$$

where L_t^{TS} and L_t^{WPP} *(kWh)* are the portions of energy sold to the external grid by the TS and WPP, respectively, S_t^{TS} and S_t^D *(kWh)* are the portions of energy purchased from the external grid by the TS and D, respectively, V_t^{PV} and V_t^{WPP} *(kWh)* are the portions sold to the district and generated by the PV panels of the TS and WPP, respectively, β and γ are the coefficients defining the minimum amount of energy to be sold to D by TS and WPP, respectively, $\tilde{E}_t^D$ (*kWh*) is the expected energy demand for D (for the moment, considered without uncertainty) at time step *t*, predicted by TS and WPP, $\tilde{V}_t^{PV}$ and $\tilde{V}_t^{WPP}$ (*kWh*) are the energy portions, which TS and WPP are ready to sell to D at time step *t.* The variables $\delta_t^{TS,ch}$, $\delta_t^{TS,dis}$, $\delta_t^{D,ch}$ *and* $\delta_t^{D,dis}$ are binary variables, which take values 0 or 1 to indicate that the battery can either only be charged or discharged at time t.

The coefficients β and γ in eqs. (A.5) and (A.20) allow regulating the energy exchanges between the microgrid agents, by imposing the minimum amount of energy that WPP and TS can supply to D under conditions of availability of wind and solar energy outputs, and promoting the local energy exchanges among the microgrid agents.

The optimization problems account for the energy balance at eqs. (A.1), (A.3), (A.10) and (A.18), and for the costs and revenues at eqs. (A.2), (A.11) and (A.19). The batteries charging and discharging dynamics is formulated with eqs. (A.6) – (A.9) for TS, and eqs. (A.12) – (A.15) for D. Eqs. (A.4), (A.16) and (A.21) are the decision variables constraints.

A.1.2. RO problem

The approach adopted in this paper allows the linear formulation of the robust counterpart of an optimization problem [17].

Train Station

Minimize $\boldsymbol{\alpha^{TS}}$

s.t.

$$-S_t^{TS} + L_t^{TS} + \delta_t^{TS,ch} \cdot R^{TS,stor} - \delta_t^{TS,dis} \cdot R^{TS,stor} + V_t^{PV} - P_t^{PV} \cdot x_t^{n+1} + E_t^{TS} \cdot x_t^{n+2} + z_t^{Power} \cdot \Gamma_t^{Power} + p_t^{P_t^{PV}} + p_t^{E_t^{TS}} \leq 0 \qquad \forall t \tag{A.22}$$

$$z_t^{Power} + p_t^{P_t^{PV}} \geq \hat{P}_t^{PV} \cdot y_t^{P_t^{PV}},\ z_t^{Power} + p_t^{E_t^{TS}} \geq \hat{E}_t^{TS} \cdot y_t^{E_t^{TS}} \qquad \forall t \tag{A.23}$$

$$-y_t^{P_t^{PV}} \leq x_t^{n+1} \leq y_t^{P_t^{PV}}, -y_t^{E_t^{TS}} \leq x_t^{n+2} \leq y_t^{E_t^{TS}} \qquad \forall t \tag{A.24}$$

$$L_t^{TS} + V_t^{PV} - P_t^{PV} \cdot x_t^{n+1} + z_t^{Micro} \cdot \Gamma_t^{Micro} + p_t^{P_t^{PV}} \leq 0 \qquad \forall t \tag{A.25}$$

$$z_t^{Micro} + p_t^{P_t^{PV}} \geq \hat{P}_t^{PV} \cdot y_t^{P_t^{PV}} \qquad \forall t \tag{A.26}$$

$$\sum_{t=0}^{T} (c_t^p \cdot S_t^{TS} - c_t^s \cdot L_t^{TS} - c_t^D \cdot V_t^{PV}) + \sum_{t=0}^{T} \left(z_t^{Cost} \cdot \Gamma_t^{Cost} + p_t^{c_t^p} + p_t^{c_t^s} + p_t^{c_t^D} \right) \leq \alpha^{TS} \tag{A.27}$$

$$z_t^{Cost} + p_t^{c_t^p} \geq \hat{c}_t^p \cdot y_t^{c_t^p}, z_t^{Cost} + p_t^{c_t^s} \geq \hat{c}_t^s \cdot y_t^{c_t^s}, z_t^{Cost} + p_t^{c_t^D} \geq \hat{c}_t^D \cdot y_t^{c_t^D} \qquad \forall t \tag{A.28}$$

$$-y_t^{c_t^p} \leq S_t^{TS} \leq y_t^{c_t^p}, -y_t^{c_t^s} \leq L_t^{TS} \leq y_t^{c_t^s}, -y_t^{c_t^D} \leq V_t^{PV} \leq y_t^{c_t^D} \qquad \forall t \tag{A.29}$$

$$S_t^{TS} \geq 0, L_t^{TS} \geq 0, V_t^{PV} \geq 0 \qquad \forall t \tag{A.30}$$

$$\begin{cases} \beta \cdot \tilde{E}_t^D \leq V_t^{PV}, & if\ P_t^{PV} \geq \beta \cdot \tilde{E}_t^D \\ 0 \leq V_t^{PV}, & otherwise \end{cases} \qquad \forall t \tag{A.31}$$

$$R_t^{TS} \leq R_{t-1}^{TS} + \delta_t^{TS,ch} \cdot R^{TS,stor} - \delta_t^{TS,dis} \cdot R^{TS,stor} \qquad \forall t \tag{A.32}$$

$$\delta_t^{TS,ch} + \delta_t^{TS,dis} \leq 1 \qquad \forall t \tag{A.33}$$

$$0 \leq \delta_t^{TS,ch} \leq 1, 0 \leq \delta_t^{TS,dis} \leq 1 \qquad \forall t \tag{A.34}$$

$$0 \leq R_t^{TS} \leq R^{TS,max}, \qquad \forall t \tag{A.35}$$

District

Minimize $\boldsymbol{\alpha^{D}}$

s.t.

$$-S_t^D - V_t^{PV} - V_t^{WPP} + (R_t^D - R_{t-1}^D) + E_t^D \cdot x_t^{n+1} + z_t^{Power} \cdot \Gamma_t^{Power} + p_t^{E_t^D} \leq 0 \quad \forall t \tag{A.36}$$

$$z_t^{Power} + p_t^{E_t^D} \geq \hat{E}_t^D \cdot y_t^{E_t^D} \qquad \forall t \tag{A.37}$$

$$-y_t^{E_t^D} \leq x_t^{n+1} \leq y_t^{E_t^D} \qquad \forall t \tag{A.38}$$

$$\sum_{t=0}^{T}\left(c_t^p \cdot S_t^D + c_t^D \cdot V_t^{WPP} + c_t^D \cdot V_t^{PV}\right) + \sum_{t=0}^{T}\left(z_t^{Cost} \cdot \Gamma_t^{Cost} + p_t^{c_t^p} + p_t^{c_t^D}\right) \leq \alpha^D \quad \text{(A.39)}$$

$$z_t^{Cost} + p_t^{c_t^p} \geq \hat{c}_t^p \cdot y_t^{c_t^p}, z_t^{Cost} + p_t^{c_t^D} \geq \hat{c}_t^D \cdot y_t^{c_t^D} \qquad \forall t \quad \text{(A.40)}$$

$$-y_t^{c_t^p} \leq S_t^D \leq y_t^{c_t^p}, -y_t^{c_t^D} \leq V_t^{WPP} + V_t^{PV} \leq y_t^{c_t^D} \qquad \forall t \quad \text{(A.41)}$$

$$R_t^D \leq R_{t-1}^D + \delta_t^{D,ch} \cdot R^{D,stor} - \delta_t^{D,dis} \cdot R^{D,stor} \qquad \forall t \quad \text{(A.42)}$$

$$\delta_t^{D,ch} + \delta_t^{D,dis} \leq 1 \qquad \forall t \quad \text{(A.43)}$$

$$0 \leq \delta_t^{D,ch} \leq 1, 0 \leq \delta_t^{D,dis} \leq 1 \qquad \forall t \quad \text{(A.44)}$$

$$0 \leq R_t^D \leq R^{D,max} \qquad \forall t \quad \text{(A.45)}$$

$$S_t^D \geq 0 \qquad \forall t \quad \text{(A.46)}$$

$$V_t^{PV} = \tilde{V}_t^{PV}, V_t^{WPP} = \tilde{V}_t^{WPP} \qquad \forall t \quad \text{(A.47)}$$

Wind Power Plant

Maximize $\boldsymbol{\alpha^{WPP}}$

s.t.

$$L_t^{WPP} + V_t^{WPP} - P_t^{WPP} \cdot x_t^{n+1} + z_t^{Power} \cdot \Gamma_t^{Power} + p_t^{P_t^{WPP}} \leq 0 \qquad \forall t \quad \text{(A.48)}$$

$$z_t^{Power} + p_t^{P_t^{WPP}} \geq \hat{P}_t^{WPP} \cdot y_t^{P_t^{WPP}} \qquad \forall t \quad \text{(A.49)}$$

$$-y_t^{P_t^{WPP}} \leq x_t^{n+1} \leq y_t^{P_t^{WPP}} \qquad \forall t \quad \text{(A.50)}$$

$$\sum_{t=0}^{T}\left(c_t^s \cdot L_t^{WPP} + c_t^D \cdot V_t^{WPP}\right) - \sum_{t=0}^{T}\left(z_t^{Cost} \cdot \Gamma_t^{Cost} + p_t^{c_t^s} + p_t^{c_t^D}\right) \geq \alpha^{WPP} \quad \text{(A.51)}$$

$$z_t^{Cost} + p_t^{c_t^s} \geq \hat{c}_t^s \cdot y_t^{c_t^s}, z_t^{Cost} + p_t^{c_t^D} \geq \hat{c}_t^D \cdot y_t^{c_t^D} \qquad \forall t \quad \text{(A.52)}$$

$$-y_t^{c_t^s} \leq L_t^{WPP} \leq y_t^{c_t^s}, -y_t^{c_t^D} \leq V_t^{WPP} \leq y_t^{c_t^D} \qquad \forall t \quad \text{(A.53)}$$

$$\begin{cases} \gamma \cdot \tilde{E}_t^D \leq V_t^{WPP}, & if\ P_t^{WPP} \geq \gamma \cdot \tilde{E}_t^D \\ 0 \leq V_t^{WPP}, & otherwise \end{cases} \qquad \forall t \quad \text{(A.54)}$$

$$L_t^{WPP} \geq 0, V_t^{WPP} \geq 0 \qquad \forall t \quad \text{(A.55)}$$

where the variables z_t^{Power}, z_t^{Cost}, z_t^{Micro} $p_t^{P_t^{WPP}}$, $p_t^{P_t^{PV}}$, $p_t^{E_t^D}$, $p_t^{E_t^{TS}}$, $p_t^{c_t^p}$, $p_t^{c_t^s}$, $p_t^{c_t^D}$, $y_t^{P_t^{WPP}}$, $y_t^{P_t^{PV}}$, $y_t^{E_t^D}$, $y_t^{E_t^{TS}}$, $y_t^{c_t^p}$, $y_t^{c_t^s}$ and $y_t^{c_t^D}$ are dual or auxiliary variables needed to formulate the linear

counterpart of the robust optimization problem [17]. These are forced to be greater than or equal to zero, similarly, x_t^{n+1} and x_t^{n+2} are auxiliary variables that are forced to be equal to one. Γ_t^{Power} and Γ_t^{Cost} define the level of uncertainty considered in each optimization model (a zero value corresponds to the deterministic problem) and are such that $0 \leq \Gamma_t^{Power} \leq 1$ and $0 \leq \Gamma_t^{Cost} \leq 2$ for the D and WPP, and $0 \leq \Gamma_t^{Power} \leq 2$ and $0 \leq \Gamma_t^{Cost} \leq 3$ for the TS. The upper limits of Γ_t^{Power} and Γ_t^{Cost} indicate the maximum number of uncertain parameters handled by the RO formulated here above. The value of the uncertainty levels can be fixed and adjusted independently by each agent depending on the uncertainty related to different numerical case studies, i.e., $\Gamma_t^{Power} = 1$ for the D and TS to account for the uncertainty in wind and PV power output in case of wind storms and associated lines failures, and $\Gamma_t^{Cost} = 2$ for D and WPP and $\Gamma_t^{Power} = 3$ for TS to account for the uncertainty in energy demands and electricity prices.

Note that the RO has the advantage that it represents the uncertainty related to the variations of the operational or environmental conditions in terms of PI without making any assumption about the probabilistic distribution on the PI. For example, for the WPP in the robust formulation the level of uncertainty $\hat{P}_t^{WPP}$ can be defined as $\hat{P}_t^{WPP} = (P_t^{WPP,ub} - P_t^{WPP,lb})/2$, where $P_t^{WPP,ub}$ and $P_t^{WPP,lb}$ (kWh) are the upper and lower prediction bounds at time t, respectively. In this work, we take the mean of the prediction interval as point estimate of the wind energy output P_t^{WPP} in eq.A.48. The point estimates of the other uncertain variables are the values calculated with the models of the individual components or other statistical data described in [22].

The robust optimization problems are solved by using the optimization package CPLEX, implemented in Java code, which guarantee global optimality for mixed integer linear programming (MIP) problems (the iterative process of optimization in CPLEX is not illustrated in the paper: the interested reader may refer to [77] for further details). After optimization, the decisions are shared among the agents through the communication process indicated in the paper.

A.2. Communication framework

Figure. A1 depicts the communication interactions among the microgrid agents. It can be noted that the microgrid does not include an independent operator, responsible for coordinating, controlling and operating the electric power system or/and market, as in most of the actual power grids. Indeed, we assume that all coordination procedures are done in a decentralized manner

through direct negotiation among the agents, similar to [10], [11]. However, to facilitate the agents communications, an additional agent called Independent System Operator (ISO) is introduced in the model, similar to [78], assisting communication between microgrid agents.

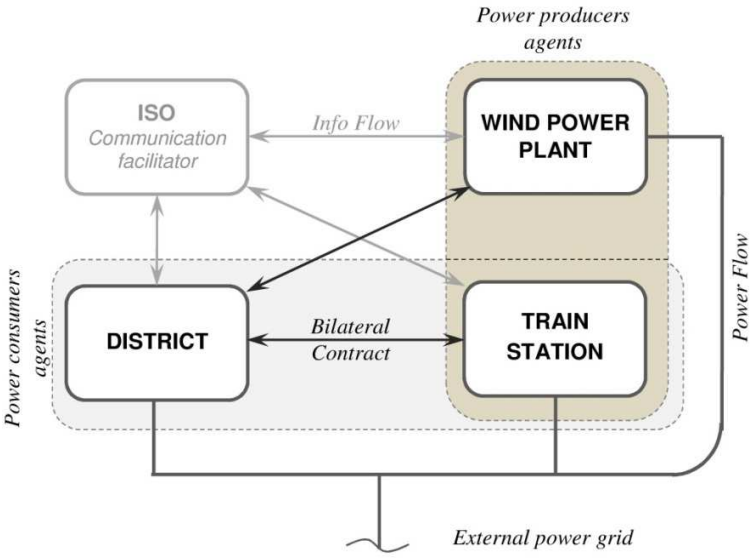

Figure. A1. Multi-layered interaction between agents [22].

The microgrid agents participate in the decision-making framework as illustrated in Figure. A2. For the sake of clarity, the hierarchy of decisions considered in this work gives priority to the energy producers, i.e., the TS and the WPP, to decide the renewable energy V_t^{PV} and V_t^{WPP} that is available to be sold to the D, and the energy quantities L_t^{PV} and L_t^{WPP} that are sold to the external grid at each time step *t*. These decisions are transmitted through the ISO agent to the D, which considers these decisions as constant parameters for its optimization problem (eqs.A.10 – A.17 and eqs.A.36 – A.47 for the deterministic problem and RO, respectively). After the determination of other energy scheduling variables, such as S_t^D and R_t^D, the D sets a bilateral agreement with the TS and the WPP in order to purchase V_t^{PV} and V_t^{WPP}, respectively. The duration of the bilateral contract is assumed to be one hour.

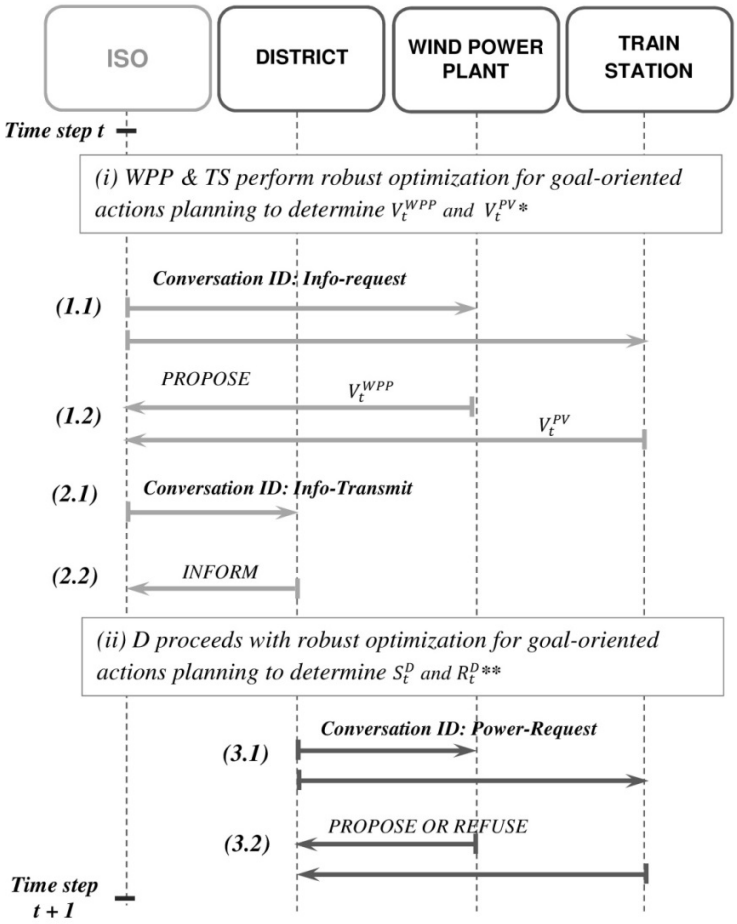

Figure. A2. Example of agents communication at time step t [22].

Table A gathers the previsions of the operational conditions (i) made by the agents themselves and (ii) received from other agents through the ISO and (iii) the decision variables.

Table A1. Previsions and decision variables.

Previsions of the operational conditions	D	WWP	TS
(i) agent personal previsions*	$E_t^D;\ c_t^p;\ c_t^D$	$P_t^{WPP};\ c_t^s;\ c_t^D$	$E_t^{TS};\ P_t^{PV};\ c_t^p;\ c_t^D;\ c_t^s$
(ii) previsions received from other agents through *ISO*	$V_t^{PV};\ V_t^{WPP}$	-	-
(iii) decision variables based on the above previsions	$S_t^D;\ R_t^D$	$V_t^{WPP};\ L_t^{WPP}$	$V_t^{PV};\ L_t^{TS};\ S_t^{TS};\ R_t^{TS}$

* Personal previsions of agents are represented by PIs for RO and point predictions for the deterministic optimization.

Note that the adopted hierarchical decision scheme allows, on the one hand, the TS and the WPP increasing their revenues by deciding which amount of energy to sell to the D or to the external

grid using the most profitable actions planning; on the other hand, it gives the possibility to the D to purchase the emissions-free and less expensive energy generated by the TS and WPP in the microgrid.

A.3. Uncertainties in energy management

The expenses and revenues of each agent, and the global reliability of the microgrid are affected by uncertain parameters, such as the energy outputs from renewable generators P_t^{PV} and P_t^{WPP}, the energy demands of the consumers E_t^{TS} and E_t^{D}, and the electricity prices c_t^{p}, c_t^{s} and c_t^{D}. This section illustrates the procedure used to account for these uncertainties.

A.3.1. Energy output of renewable energy generators

The energy outputs from the renewable generators are affected by the variability of the renewable sources of energy, i.e., wind for WPP and solar irradiation for PV.

As discussed previously, the uncertainty related to the availability of the wind energy output P_t^{WPP} is described by prediction intervals (PIs), estimated by a multi-perceptron neural network (NN) [27]. The PIs are optimized in terms of maximum Coverage Probability (CP) and minimum Prediction Interval Width (PIW). A multi-objective genetic algorithm (namely, non-dominated sorting genetic algorithm–II (NSGA-II)) is used to find the optimal parameters (weights and biases) of the NN. Pareto-optimal solution sets of several non-dominated solutions with respect to the two objectives (CP and PIW), are generated.

As presented in Section 3, the expected value of PV energy output P_t^{PV} is simulated based on the solar irradiation and technical specification of PV module [33], [34]. In absence of a prediction model for the PV energy output, the related uncertainty is described by intervals, whose lower and upper bounds are symmetric around the expected value of PV energy output. The width of the interval is selected to account for the variability of the PV energy output in the time period considered.

The actual energy output of renewable generators is also affected by mechanical failures, which may lead to periods of production unavailability during the subsequent repairs. A description of this effect is given by the compound quantitative indicator called technical unavailability [79]. Mechanical failures of generation units of the same type are, for simplicity, assumed to be independent from each other: no common causes for failures are considered. Moreover, no particular reduction of energy production due to units degradation has been considered: only two

states are possible, i.e., 100% of technical availability and 0% during the repair upon a failure. Failure and repair times are assumed to follow exponential distributions, considering the useful life of the components. For the numerical application of this paper, the Mean Time To Failure (MTTF) and Mean Time To Repair (MTTR) of the wind energy generation units have been taken equal to 1920 *h* and 25 *h*, respectively [80]. The failures of the power electronics parts are major contributors to the reliability problem and represent about 40% of the annual failure frequency for the wind turbines, based on long-term feedback experience [44], which is almost two times higher than the annual frequency of other wind turbine components. For the sake of simplicity, in this research we used the term 'mechanical failure' to represent all types of failures of the wind turbines and the generators.

Failure times and repair durations are simulated by sampling from the exponential distribution of failure and repair times for the given MTTF and MTTR values, with the inverse transform technique [81].

A.3.2. Energy demand

Similar to the wind energy output, PIs accounting for the variability of the energy demands E_t^{TS} and E_t^D, are used as estimated a GA – trained Neural Network (NN) [27].

A.3.3. Electricity prices

Similar to the PV energy output, the uncertainty related to the variability of electricity prices c_t^p, c_t^s and c_t^D is accounted for in the form of intervals, whose lower and upper bounds are symmetric around the expected value of each variable. The width of the intervals is selected to account for the fluctuations of these variables in the time period considered.

Bibliography

[1] J. C. Glenn, T. J. Gordon, and E. Florescu, "2009 State of the Future," 2009.

[2] B. J. Owen, "The planet 's future : Climate change ' will cause civilisation to collapse '," *The Independent*, London, 2009.

[3] N. D. Hatziargyriou, *European Transactions on Electrical Power. Special Issue: Microgrids and Energy Management*, no. December 2010. 2011.

[4] A. G. De Muro, J. Jimeno, and J. Anduaga, “Architecture of a microgrid energy management system,” *Eur. Trans. Electr. Power*, vol. 21, pp. 1142–1158, 2011.

[5] E. Kuznetsova, K. Culver, and E. Zio, “Complexity and vulnerability of Smartgrid systems,” in *European Safety and Reliability Conference (ESREL 2011)*, 2011, pp. 1–8.

[6] M. H. Colson, C. M. Nehrir, and R. W. Gunderson, “Multi-agent Microgrid Power Management,” in *18th IFAC World Congress*, 2011, pp. 3678–3683.

[7] P. P. Reddy and M. M. Veloso, “Strategy Learning for Autonomous Agents in Smart Grid Markets,” in *Twenty-Second International Joint Conference on Artificial Intelligence*, 2005, pp. 1446–1451.

[8] T. Krause, E. Beck, R. Cherkaoui, A. Germond, G. Andersson, and D. Ernst, “A comparison of Nash equilibria analysis and agent-based modelling for power markets,” *Int. J. Electr. Power Energy Syst.*, vol. 28, no. 9, pp. 599–607, Nov. 2006.

[9] A. Weidlich and D. Veit, “A critical survey of agent-based wholesale electricity market models,” *Energy Econ.*, vol. 30, no. 4, pp. 1728–1759, Jul. 2008.

[10] S. Yousefi, M. P. Moghaddam, and V. J. Majd, “Optimal real time pricing in an agent-based retail market using a comprehensive demand response model,” *Energy*, vol. 36, no. 9, pp. 5716–5727, Sep. 2011.

[11] Z. Jun, L. Junfeng, W. Jie, and H. W. Ngan, “A multi-agent solution to energy management in hybrid renewable energy generation system,” *Renew. Energy*, vol. 36, no. 5, pp. 1352–1363, May 2011.

[12] E. Kuznetsova, C. Ruiz, Y. F. Li, E. Zio, G. Ault, and K. Bell, “Reinforcement learning for microgrid energy management,” *Energy*, vol. 59, pp. 133–146, 2013.

[13] Y. Zeng, Y. Cai, G. Huang, and J. Dai, “A Review on Optimization Modeling of Energy Systems Planning and GHG Emission Mitigation under Uncertainty,” *Energies*, vol. 4, no. 12, pp. 1624–1656, Oct. 2011.

[14] J. Lagorse, M. G. Simoes, and A. Miraoui, “A Multiagent Fuzzy-Logic-Based Energy Management of Hybrid Systems,” *Ind. Appl. IEEE Trans.*, vol. 45, no. 6, pp. 2123–2129, 2009.

[15] J. Solano Martínez, R. I. John, D. Hissel, and M.-C. Péra, “A survey-based type-2 fuzzy logic system for energy management in hybrid electrical vehicles,” *Inf. Sci. (Ny).*, vol. 190, pp. 192–207, May 2012.

[16] A. Ben-Tal and A. Nemirovski, “Robust solutions of uncertain linear programs,” *Oper. Res. Lett.*, vol. 25, no. 1, pp. 1–13, Aug. 1999.

[17] D. Bertsimas and M. Sim, “The Price of Robustness,” *Oper. Res.*, vol. 52, no. 1, pp. 35–53, 2004.

[18] V. Krey, D. Martinsen, and H.-J. Wagner, “Effects of stochastic energy prices on long-term energy-economic scenarios,” *Energy*, vol. 32, no. 12, pp. 2340–2349, Dec. 2007.

[19] Y. P. Cai, G. H. Huang, Z. F. Yang, Q. G. Lin, and Q. Tan, “Community-scale renewable energy systems planning under uncertainty—An interval chance-constrained programming approach,” *Renew. Sustain. Energy Rev.*, vol. 13, no. 4, pp. 721–735, May 2009.

[20] M. Liu, “An Interval-parameter Fuzzy Robust Nonlinear Programming Model for Water Quality Management,” *J. Water Resour. Prot.*, vol. 05, no. 01, pp. 12–16, 2013.

[21] Y. Li and G. Huang, “Robust interval quadratic programming and its application to waste management under uncertainty,” *Environ. Syst. Res.*, vol. 1, no. 1, p. 7, 2012.

[22] E. Kuznetsova, C. Ruiz, Y. F. Li, and E. Zio, “Reliable microgrid energy management under environmental uncertainty and mechanical failures: an agent-based modeling and robust optimization,” in *Safety, Reliability and Risk Analysis: Beyond the Horizon (ESREL 2013)*, 2013, pp. 2873 – 2882.

[23] A. Parisio, C. Del Vecchio, and A. Vaccaro, “Electrical Power and Energy Systems A robust optimization approach to energy hub management,” *Int. J. Electr. Power Energy Syst.*, vol. 42, no. 1, pp. 98–104, 2012.

[24] C. Chen, Y. P. Li, G. H. Huang, and Y. F. Li, “A robust optimization method for planning regional-scale electric power systems and managing carbon dioxide,” *Electr. Power Energy Syst.*, vol. 40, pp. 70–84, 2012.

[25] C. Chen, Y. P. Li, G. H. Huang, and Y. Zhu, “An inexact robust nonlinear optimization method for energy systems planning under uncertainty,” *Renew. Energy*, vol. 47, pp. 55–66, 2012.

[26] A. Khosravi, S. Nahavandi, D. Creighton, and F. A. Amir, “A Comprehensive Review of Neural Network-based Prediction Intervals and New Advances,” *IEEE Trans. Neural Net.*, vol. 22, no. 9, pp. 1341–1356, 2011.

[27] R. Ak, Y. F. Li, V. Vitelli, and E. Zio, “Multi-objective Generic Algorithm Optimization of a Neural Network for Estimating Wind Speed Prediction Intervals,” *Submitt. to Appl. Soft Comput.*, 2013.

[28] European Commission, “Photovoltaic Solar Energy Best Practice Stroies,” 2002.

[29] E. Fischer and C. Lo, “Back to the future : Top trends in railway station design,” *railway-technology.com*, 2011. [Online]. Available: http://www.railway-

technology.com/features/featureback-to-the-future-top-trends-in-railway-station-design. [Accessed: 24-Sep-2013].

[30] RTE, “Bilan électrique 2012,” 2012.

[31] L. Al-Sharif, “Modelling of escalator energy consumption,” *Energy Build.*, vol. 43, no. 6, pp. 1382–1391, Jun. 2011.

[32] Ademe, “Eclairage public: routier, urban, grands espaces, illuminations et cadre de vie,” 2002.

[33] F. A. Mohamed and H. N. Koivo, “System modelling and online optimal management of MicroGrid using mesh adaptive direct search,” *Int. J. Electr. Power Energy Syst.*, vol. 32, no. 5, pp. 398–407, 2010.

[34] Y. M. Atwa, M. M. A. Salama, and R. Seethapathy, “Optimal renewable resources mix for distribution system energy loss minimization,” *IEEE Trans. Power Syst.*, vol. 25, no. 1, pp. 360–370, 2010.

[35] D. C. Hill, D. Mcmillan, K. R. W. Bell, and D. Infield, “Application of auto-regressive models to UK wind speed data for power system impact studies,” *IEEE Trans. Sustain. Energy*, vol. 3, no. 1, 2012.

[36] E. N. Dialynas and A. V. Machias, “Reliability modelling interactive techniques of power systems including wind generating units,” *Arch. fur Elektrotechnik*, vol. 72, pp. 33 – 41, 1989.

[37] C. Fong, S. Haddad, and D. Patton, “The IEEE reliability test system - 1996,” *IEEE Trans. Power Syst.*, vol. 14, no. 3, 1999.

[38] EEX, “Hour Contracts - France,” *European Energy Exchange*, 2013. [Online]. Available: http://www.eex.com/en/Market Data/Trading Data/Power/Hour Contracts | Spot Hourly Auction/spot-hours-table/2013-02-14/FRANCE. [Accessed: 13-Feb-2013].

[39] E. Kuznetsova, Y.-F. Li, C. Ruiz, and E. Zio, “An integrated framework of agent-based modelling and robust optimization for microgrid energy management,” *Appl. Energy*, vol. 129, pp. 70 – 88, 2014.

[40] G. Tamizhmani, “Testing the reliability and safety of photovoltaic modules: failure rates and temperature effects,” *Photovoltaics Int. J.*, pp. 146 – 152, 2009.

[41] U. Jahn and T. Ü. V Rheinland, “PV Module Reliability Issues Including Testing and Certification,” Frankfurt, Germany, 2012.

[42] B. R. G. Lucas, “Lessons Learned and Challenges for Implementing Infrared Thermography and Systems Analysis in Large PV Solar Plant Arrays,” 2013.

[43] F. Ancuta and C. Cepisca, “Failure Analysis Capabilities for PV Systems,” *Recent Res. Energy, Environ. Entrep. Innov.*, pp. 109–115, 2011.

[44] B. Hahn, M. Durstewitz, and K. Rohrig, “Reliability of Wind Turbines Break down of Wind Turbines,” in *Wind Energy*, Springer B., 2007, pp. 329–332.

[45] P. Tavner, Y. Qiu, A. Korogiannos, and Y. Feng, “The correlation between wind turbine turbulence and pitch failure,” UK, 2010.

[46] C. Su, Q. Jin, and Y. Fu, “Correlation analysis for wind speed and failure rate of wind turbines using time series approach,” *J. Renew. Sustain. Energy*, vol. 4, no. 3, p. 032301, 2012.

[47] K. Alvehag and L. Söder, “A Reliability Model for Distribution Systems Incorporating Seasonal Variations in Severe Weather,” *IEEE Trans. Power Deliv.*, vol. 26, no. 2, pp. 910–919, 2011.

[48] C. Lallemand, “Methodology for a Risk Based Asset Management,” Royal Institute of Technology, 2008.

[49] B. B. Brabson and J. P. Palutikof, “Tests of the Generalized Pareto Distribution for Predicting Extreme Wind Speeds,” *J. Appl. Meteorol. Climatol.*, vol. 39, no. 9, pp. 1627–1640, 2000.

[50] D. York, M. Kushler, and P. Witte, “Examining the Peak Demand Impacts of Energy Efficiency: A Review of Program Experience and Industry Practices,” Washington, USA, 2007.

[51] F. Stern, “Chapter 10: Peak Demand and Time-Differentiated Energy Savings Cross-Cutting Protocols,” in *The Uniform Methods Project: Methods for Determining Energy Efficiency Savings for Specific Measures*, no. April, 2013, pp. 1 – 13.

[52] J. Protasiewicz and P. S. Czczepaniak, “Neural Models of Demands for Electricity - Prediction and Risk Assessment,” *Electr. Rev.*, vol. 88, no. 6, pp. 272–279, 2012.

[53] S. Heiken, D. Elzinga, S.-K. Kim, and Y. Ikeda, “Impact of Smart Grid Technologies on Peak Load to 2050,” Paris, France, 2011.

[54] C. Sigauke, A. Verster, and D. Chikobvu, “Tail Quantile Estimation of Heteroskedastic Intraday Increases in Peak Electricity Demand,” *Open J. Stat.*, vol. 02, no. 04, pp. 435–442, 2012.

[55] R. J. Hyndman and S. Fan, “Forecasting long-term electricity demand for,” Melbourne, Australia, 2009.

[56] E. Chiodo and D. Lauria, “Probabilistic description and prediction of electric peak power demand,” *Electrical Systems for Aircraft, Railway and Ship Propulsion (ESARS), 2012*. pp. 1–7, 2012.

[57] ERCOT, “2013 ERCOT Planning Long-Term Hourly Peak Demand and Energy Forecast,” 2013.

[58] P. E. McSharry, S. Bouwman, and G. Bloemhof, “Probabilistic Forecasts of the Magnitude and Timing of Peak Electricity Demand,” *IEEE Trans. Power Syst.*, vol. 20, no. 2, pp. 1166–1172, May 2005.

[59] C. J. Ziser, Z. Y. Dong, and T. Saha, “Investigation of Weather Dependency and Load Diversity on Queensland Electricity Demand,” in *Australasian Universities Power Engineering Conference*, 2005, pp. 25–28.

[60] Y. Yu and L. Zhang, “An empirical study on seasonal fluctuations in electricity demand in China,” *J. Renew. Sustain. Energy*, vol. 4, no. 3, p. 031803, 2012.

[61] H. Ren and W. Gao, “A MILP model for integrated plan and evaluation of distributed energy systems,” *Appl. Energy*, vol. 87, no. 3, pp. 1001–1014, 2010.

[62] W. Saman and E. Halawa, “NATHERS - Peak Load Performance Module Research,” Canberra, Australia, 2009.

[63] DECC, “Estimated impacts of energy and climate change policies on energy prices and bills,” London, England, 2013.

[64] J. Faith, “Regional variations in energy prices revealed,” *YourMoney.com*, 2013. .

[65] R. Mena, M. Hennebel, Y.-F. Li, C. Ruiz, and E. Zio, “A Risk-Based Simulation and Multi-Objective Optimization Framework for the Integration of Distributed Renewable Generation and Storage,” *Renew. Sustain. Energy Rev.*, vol. 37, pp. 778–793, 2014.

[66] H. Falaghi, C. Singh, M.-R. Haghifam, and M. Ramezani, “DG integrated multistage distribution system expansion planning,” *Int. J. Electr. Power Energy Syst.*, vol. 33, no. 8, pp. 1489–1497, Oct. 2011.

[67] Smartgrid.gouv, “Critical Peak Pricing Lowers Peak Demands and Electric Bills in South Dakota and Minnesota,” 2013. [Online]. Available: http://www.smartgrid.gov/case_study/news/critical_peak_pricing_lowers_peak_demands_and_electric_bills_south_dakota_and_minnesota. [Accessed: 29-Nov-2013].

[68] K. Herter, P. McAuliffe, and A. Rosenfeld, “An exploratory analysis of California residential customer response to critical peak pricing of electricity,” *Energy*, vol. 32, no. 1, pp. 25–34, Jan. 2007.

[69] A. Bego, L. Li, and Z. Sun, “Identification of reservation capacity in critical peak pricing electricity demand response program for sustainable manufacturing systems,” *Int. J. Energy Res.*, p. n/a–n/a, 2013.

[70] Y. G. Hegazy, M. M. A. Salama, and A. Y. Chikhani, “Adequacy assessment of distributed generation systems using Monte Carlo simulation,” *IEEE Trans. Power Syst.*, vol. 18, no. 1, pp. 48–52, 2003.

[71] P. J. Luickx, P. S. Pérez, J. Driesen, and W. D. D’haeseleer, “Imbalance Tariff Systems In European Countries And The Cost Effect Of Wind Power,” WP EN2009-002, 2009.

[72] P. Pinson, C. Chevallier, and G. N. Kariniotakis, “Trading Wind Generation From Short-Term Probabilistic Forecasts of Wind Power,” *IEEE Trans. Power Syst.*, pp. 1–9, 2007.

[73] J. Usaola, O. Ravelo, G. González, F. Soto, M. C. Dávila, and B. Díaz-Guerra, “Benefits for Wind Energy in Electricity Markets from Using Short Term Wind Power Prediction Tools - a Simulation Study,” *Wind Eng.*, vol. 28, no. 1, pp. 119–127, Jan. 2004.

[74] H.-M. Kim, Y. Lim, and T. Kinoshita, “An Intelligent Multiagent System for Autonomous Microgrid Operation,” *Energies*, vol. 5, no. 12, pp. 3347–3362, Sep. 2012.

[75] R. C. Garcia, J. Contreras, M. Van Akkeren, and J. B. C. Garcia, “A GARCH Forecasting Model to Predict Day-Ahead Electricity Prices,” *IEEE Trans. Power Syst.*, vol. 20, no. 2, pp. 867–874, 2005.

[76] M. Cococcioni, E. D’Andrea, and B. Lazzerini, “24-hour-ahead forecasting of energy production in solar PV systems,” in *Intelligent Systems Design and Applications (ISDA), 2011 11th International Conference on*, 2011, pp. 1276–1281.

[77] IBM, “IBM ILOG CPLEX Optimization Studio, CPLEX User’s Manual,” 2011.

[78] Z. Zhi, C. Wai Kin, and C. Joe H, “Agent-based simulation of electricity markets : a survey of tools,” *Artif. Intell. Rev.*, vol. 28, pp. 305–342, 2009.

[79] G. M. J. Herbert, S. Iniyan, and R. Goic, “Performance , reliability and failure analysis of wind farm in a developing country,” *Renew. Energy*, vol. 35, no. 12, pp. 2739–2751, 2010.

[80] R. Karki and R. Billinton, “Reliability/cost implications of PV and wind energy utilization in small isolated power systems,” *IEEE Trans. Energy Convers.*, vol. 16, no. 4, pp. 368–373, 2001.

[81] E. Zio, *The Monte Carlo Simulation Method for System Reliability and Risk Analysis*. Springer, 2013.